Naval Research Reviews

Office of Naval Research
Four / 1988 – One / 1989
Vol XL / XLI

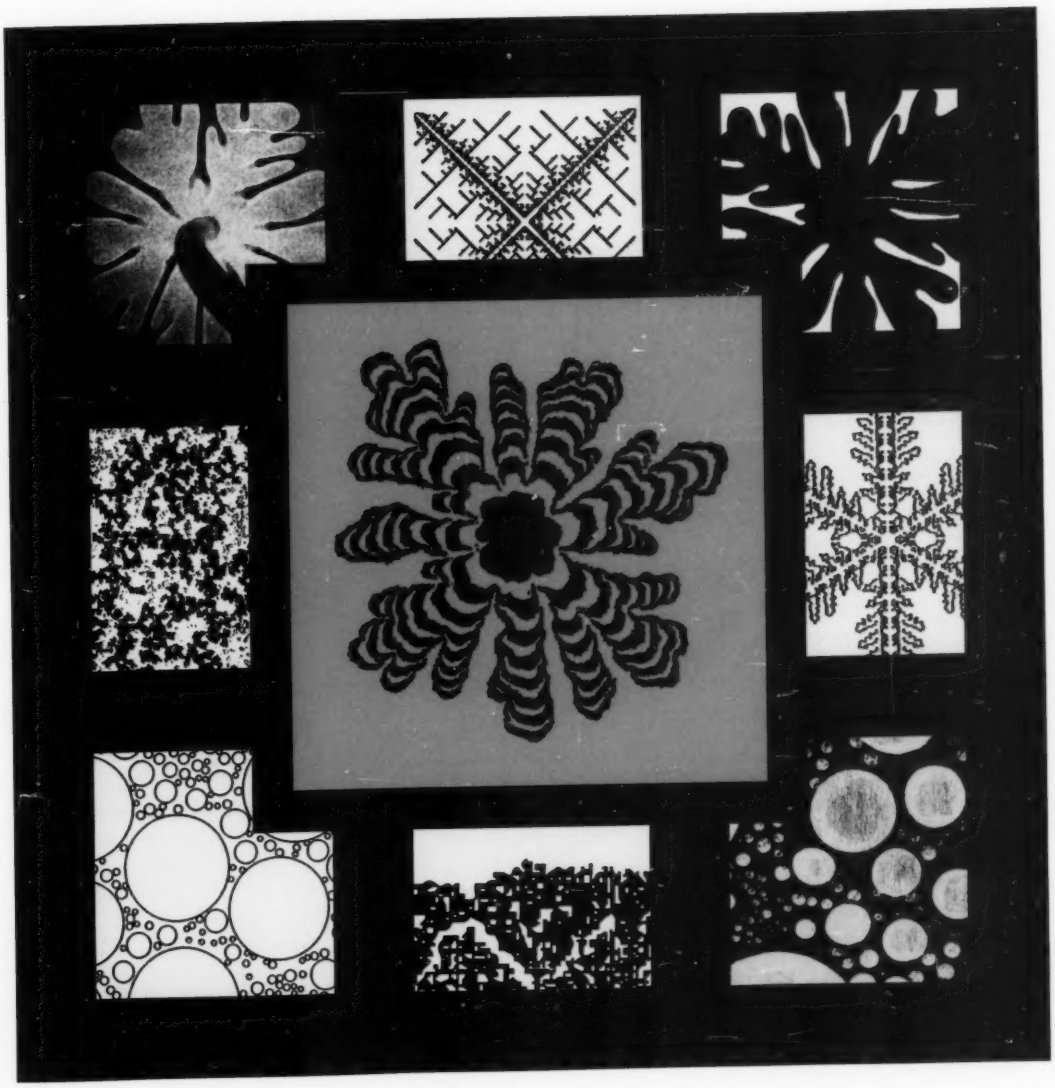

Ocean Floor Topography

Oceanographer Marie Tharp is shown in this photo from the early 1950's at her drawing board detailing one of her famous geophysical charts of the sea floor. She has been associated with Lamont-Doherty Geological Observatory, Columbia University, since its founding in 1949 until retiring in 1983. During this time she collaborated with the late Dr. Bruce C. Heezen in the study of sea floor topography; this work was funded by the Office of Naval Research for many years. In 1977 their studies resulted in the famous World Ocean Floor Panorama. This pictorial representation of the sea floor is based on more than 5,000,000 miles of soundings taken by oceanographic institutions and hydrographic bureaus of many countries and the bathymetric studies by Dr. Heezen and Marie Tharp. The chart remains today a standard for its accuracy in depicting the features of the ocean floor.

For sale by the Superintendent of Documents, U.S. Government Printing Office, Washington, D.C. 20402

Figure 2:

Sierpinski gasket is a regular fractal made up of triangles. One starts with a single triangle. In the next step, three triangles are put together to form a new triangle with a triangle missing in the middle. In the next generations, again three of the new triangles are put together to form a larger triangle with a triangle missing in the middle. Clearly this process can be continued ad infinitum to form a very large pattern. Since the repeating unit is always of the form of three triangles with a missing triangle in the middle, this object is self-similar at any length scale. The fractal dimension of a Sierpinski gasket is D=log3/log2=1.58. . . .

In contrast, fractal shapes and patterns found in nature are usually random fractals. The reason is that they consist of random shapes or patterns that appear stochastically at any length scale. Because of this randomness their self-similarity is only statistical. Another property of natural fractals is that their self-similarity extends only over a finite range, for example from atomic sizes to the maximum length in the system. Examples of random fractals include such objects as the coastlines and mountains, mentioned earlier as well as many disordered materials like polymers, colloids and gels. In fact, much of the current activity in the application of fractal concepts to physical systems has been in the area of random materials.[2]

The fractal dimension of an object or a pattern serves to characterize it and often indicates the manner in which it has been formed. There are several ways to determine the fractal dimension, but one of the most widely used methods is to relate the size of the object to its length. Let us consider the Sierpinski gasket shown in Figure 2. In each generation of the Sierpinski gasket, the length of the new triangle is 2 times the length of the previous one, and its mass is 3 times the previous mass. In contrast, if we construct a non-fractal object, like a regular triangle, then every time its length is doubled, its mass is quadrupled. If the length of a regular triangle is increased by a factor of n, then its mass would be $n^2M(r)$, where r is the length of the original triangle and $M(r)$ is its mass. The number 2 is the dimension of the object; a trivial result for a regular two dimensional triangle.

In general, the fractal dimension is the exponent or power to which n is raised. The fractal dimension D is defined by the relation, $M(nr)=n^DM(r)$, where $M(nr)$ is the mass after the length has been scaled by a factor of n. For the Sierpinski gasket $M(2r)=3M(r)$, because every time r is doubled, the mass is tripled. Therefore, the fractal dimension D of a Sierpinski gasket can be determined from the relation, $3=2^D$, which implies that $D=\log3/\log2=1.58\ldots$. This method can be used to determine the fractal dimension of any object or pattern. In the case of a random fractal, one can simply draw circles of increasing radii about a point on the object and determine the mass $M(r)$ within a circle of radius r and compare it with the mass within a circle of radius nr. The fractal dimension D can be calculated from the relation $M(nr)=n^DM(r)$, as before.

Time can also be fractal. Let us assume that we use a certain fixed time interval to make a standard measurement of time. This could be, for example, beeps recorded on a magnetic tape every one second. We can tell time by this device no matter how fast or slow the tape is played. If the tape is played at twice the speed, the time between beeps is half a second; if it is played at half the speed, the time interval is two seconds, and so on. Now, imagine a process consisting of events or beeps that is fractal in time. In such a process there is no characteristic time between beeps. If we make a recording of the events in this process and we play the tape at any speed, we find beeps at all possible time intervals: from the shortest time that we can measure between two beeps to as long as we listen to the tape. There is no fixed or characteristic time interval that we could use as a standard to measure the time between beeps. We cannot use the average time between beeps either, because it depends on the length of time that we listen to the tape. This is the distinguishing feature of a distribution of times that is fractal. The reason is that for a random distribution of time intervals, the average time is always constant. No matter how long we listen to the tape, the mean time between the beeps is the same. Processes with a fractal time distribution occur commonly in nature; the best example is 1/f noise.

In the following, I will briefly discuss some of my recent work on the development and application of fractal concepts in physical systems which have been supported by the Office of Naval Research. Despite the limited scope of this review, I think it should give an indication of the richness and complexity of the phenomena that can be understood using the mathematical tools of fractal geometry.

Percolation and Gelation

Many materials of technological and practical importance have an inhomogeneous, disordered structure somewhere between ordered crystals and random gases. Examples include the gelation of polymeric materials[2] and the growth of clusters on surfaces via atomic chemisorption, composite mixtures of conducting and dielectric materials, and dilute magnets. The formation of this type of system can be described by a growth process in which individual elements randomly join together to form an interconnected, percolating network.[3,4] The most widely used model for such systems is the percolation model, in which sites (or bonds) on a lattice are occupied randomly with a probability p, independent of the occupation of the neighboring sites. Nearest-neighbor sites are then considered to be connected, resulting in clusters of varying sizes and geometries. If the probability p is large enough, $p>p_c$, one cluster will percolate through the entire lattice. This "infinite" cluster corresponds to a gel in gelation, or to a conduction path through metallic atoms in a mixture of conducting and dielectric materials. Its formation at the percolation threshld p_c signals a geometric phase transition, and it is well established that in the region around p_c random percolation exhibits scale-invariance and fractal behavior. In particular, the percolating cluster at the percolation threshold is a fractal object, with holes and irregularities at all length scales.

In general, however, a physical system will have some type of interaction between its individual elements.[3] In surface deposition, for example, the presence of neighbors can either enhance or deter absorption at a site. Such interactions will give rise to correlations which can affect the properties of the system in important ways. We have introduced and investigated an interactive percolation model which is a simple generalization of random percolation.[3,4] Instead of using a single probability p to decide if a site should be occupied, two probabilities are used, p_0 and p_1, according to whether the site has no neighbors or at least one neighbor, respectively. The value of the percolation threshold p_c and other properties of the system depend on the parameter $r=p_1/p_0$. For $r=1$, the system corresponds to random percolation. When $r>1$, the site occupation will be "ferromagnetic" in nature, since sites that have occupied neighbors will be preferred over those that do not. Cluster nucleation will be small, resulting in widely separated clusters. Eventually, these compact clusters, or "blobs", link together and form large, fractal clusters, one of which will percolate through the system. This can be observed in Figure 3, which shows the distribution of clusters at the percolation threshold for several values of r. When $r<1$, on the other hand, the site occupation will be "antiferromagnetic" in nature, since the presence of occupied neighbors will be inhibitory. Initially, therefore, there will be many single-particle blobs, which will only link together with difficulty. They will tend to lie on one of two sublattices, forming next-nearest-neighbor-connected domains separated by antiphase boundaries.

At first glance, the percolative structures shown in Figure 3 appear to be very different from each other. Consider, however, when the value of r is large, and instead of the original particles, the blobs are taken to be the basic elements which join together to form percolating clusters. Then, these pictures are very similar to random percolation (on a smaller lattice). This suggests that as long as all quantities are scaled by the linear size of these blobs, the properties of the system will not change. We have made extensive investigations of the properties of the interacting percolation model. We find that our data for all finite r are consistent with the idea that the fractual dimension and other properties of the interactive percolation model are the same as random percolation. Thus, the interactions introduce correlations that are significant only on length scales smaller than the blob size.

Fractal Distribution of Clusters

The formation of a distribution of various size clusters is the characteristic feature of numerous processes in physics, chemistry, biology, and engineering. Despite the fact that the formation of clusters, from atomic clusters to a distribution of galaxies, had been a subject of intensive investigations for many decades, no unified description of these processes existed. Thus, the recent development that the distribution of clusters is scale-invariant[5-8] and can be described by fractal concepts has opened the way for important new developments which are leading to a unified description of many cluster-growth processes.[2,5-18]

In general, cluster formation can be divided into two classes depending on whether the clusters have a ramified, fractal structure or are smooth and spherical like liquid droplets. Fractal clusters are generally found in aggregation processes[2,5-15] involving small particles, which include colloids, aerosols, polymers, and many biological processes. In contrast, droplet growth[16-18] is observed when the coalescing clusters are in the liquid state, such as the formation of vapor-deposited thin films, breath figures, clouds, rain, fog, foam, and froth. Figure 4 shows an example of a model of cluster growth by diffusion limited aggregation[2] which leads to the formation of a distribution of fractal clusters. In this process the system initially consists of a fixed number of monomers which diffuse and interact to form larger clusters. Experiments and simulations have shown that large aggregates have a fractal geometry with a dimensionality $D\sim1.4$ in two dimensions and $D\sim1.8$ in three dimensions.

Figure 3:

Sample cluster distribution at the percolation threshold in the interactive percolation model for various values of r. The percolating cluster is black; all others are gray. For r=1, the system corresponds to random percolation. When r>1, cluster nucleation will be small, resulting in widely separated clusters. When r<1, the presence of occupied neighbors will be inhibitory. Initially, therefore, there will be many single-particle blobs, which will only link together with difficulty. They will tend to lie on one of two sublattices, forming next-nearest-neighbor-connected domains separated by antiphase boundaries. [From ref. 3]

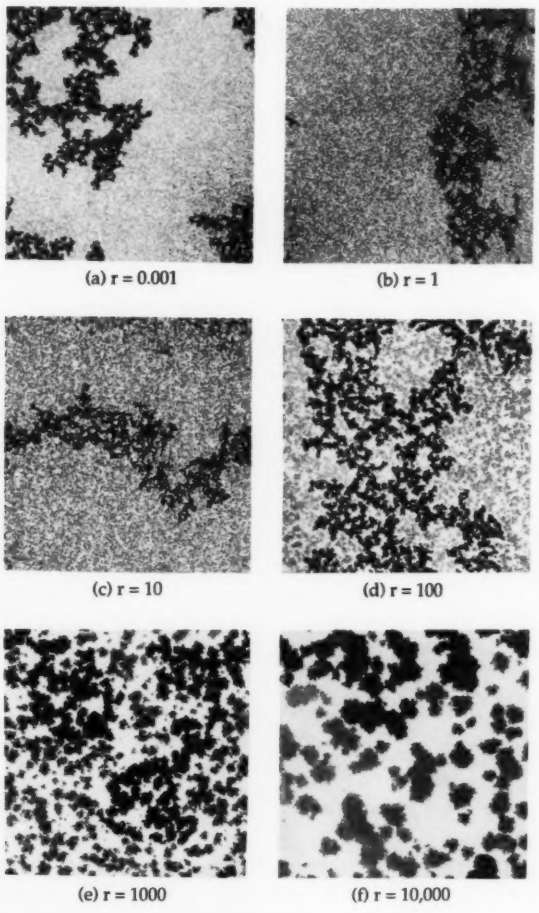

(a) r = 0.001 (b) r = 1

(c) r = 10 (d) r = 100

(e) r = 1000 (f) r = 10,000

Figure 4:

Evolution of the cluster size distribution in a diffusion-limited aggregation process. The system is initially composed of a fixed number of monomers. The monomers and clusters diffuse and join together to form larger clusters. The fractal dimension of the large clusters in two dimensions is ~1.4. [From ref. 11]

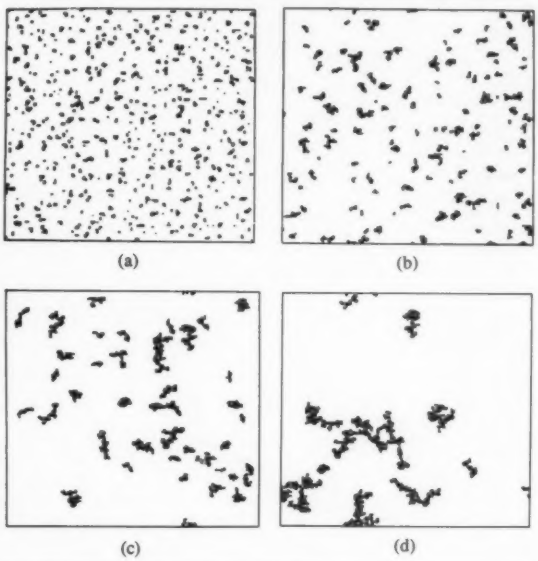

(a) (b)

(c) (d)

There are many processes in which spherical droplets grow by absorption or condensation of smaller droplets or atoms.[16-18] An example of the formation of a distribution of regular shape droplets is shown in Figure 5, which is an SEM micrograph of tin vapor deposited on a sapphire substrate.[16] In this type of experiment[16] the substrate is held at a temperature slightly higher than the melting temperature of the deposited material. Since the deposited material is in a liquid state, it forms spherical (or hemispherical) droplets on the surface which grow and coalesce to form a distribution of droplets. The smooth shape of the droplets is preserved throughout the growth process, because when two or more droplets touch, they coalesce to form a new droplet with mass conservation. An example of distribution of droplets obtained in computer simulation of a simple model of droplet growth is also shown in Figure 5. The agreement between the results of the simulations (right) and the experiments (left) indicates that our model captures the essential features of droplet growth in thin film experiments.

Figure 5:

SEM micrograph of tin vapor deposited on a sapphire substrate is shown on the right and the distribution of droplets obtained by computer simulation of a simple model of droplet growth is shown on the left. There are many qualitative similarities between these pictures and we have also shown quantitatively that the model captures many of the essential features of droplet growth in thin film experiments. [From ref. 16]

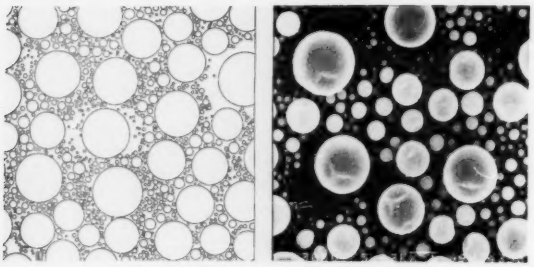

The significant result of these studies is that the distribution of both fractal clusters in such processes as colloidal aggregation and smooth droplets in the growth of thin films or breath figures are self-similar and can be described by fractal concepts.[15-18] In particular, using the dynamic scaling theory,[15-18] we have shown that the cluster size distribution is self-similar in both time and space. This implies that the cluster size distributions obtained at different times look the same if time and length are properly scaled. For example, Figure 6 demonstrates the self-similarity of cluster size distribution in both aggregation and droplet growth processes. In each case the distributions for various times are shown to collapse to a single "universal" curve when they are scaled according to the dynamic scaling theory. This type of self-similarity has been shown to exist in a wide variety of systems, including colloids, aggregates and droplets.

Figure 6:

Self-similarity of cluster size distribution in aggregation and droplet growth processes. In each graph the distributions for various times are found to collapse to a single curve when they are scaled according to the dynamic scaling theory. This type of self-similarity has been verified in a wide variety of theoretical and experimental systems, including colloids, aggregates and droplets. [From ref. 9 and 12]

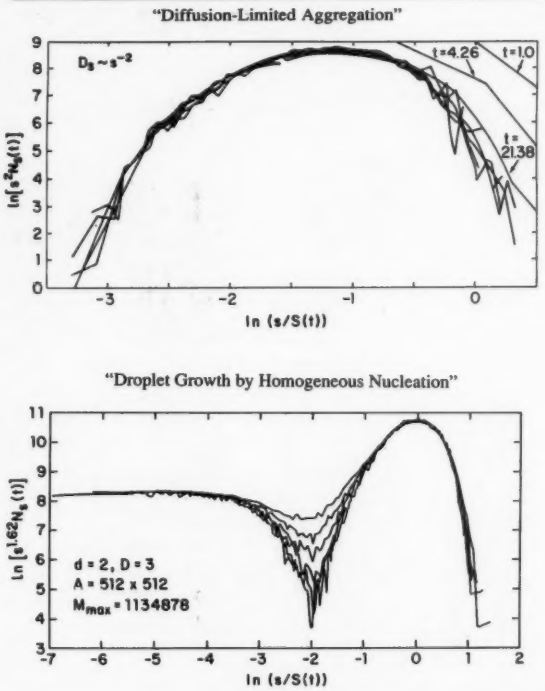

Rough Surfaces: Self-affine Fractals

The formation of complex structures and patterns is common in a wide variety of physical, chemical and biological processes, including crystal growth, solidification, aggregation, vapor deposition, and combustion. The most characteristic feature of these patterns is the existence of an evolving interface separating the structure from the outside. Thus, one way to develop a better understanding of growth phenomena would be to study the dynamics of the interface.[19-21] Surface properties play an important role in scientific and industrial applications as well. Therefore, characterization of surface roughness is a problem of considerable practical importance.

We have studied the evolution of the interface in a number of models which simulate growth by vapor deposition or sedimentation.[19-21] In this class of models we let particles simply rain down and stick to a surface. Newly arriving particles stick and become part of the aggregate when they reach a particle that is already part of the deposit. Two examples of the type of surfaces found in these simulations are shown in Figure 7. In the process on the right we have incorporated the effects of local diffusion by allowing a newly arriving particle to diffuse on the surface until it comes to rest at a local surface minima. This effect which tends to smooth the sur-

Figure 7:

Two types of deposits and interfaces that are found in the simulations of models of thin film growth by vapor deposition or sedimentation are shown here. In this class of models particles simply rain down and stick to a surface. Newly arriving particles stick and become part of the cluster when they reach a particle that is already part of the deposit. In the process on the right particles fall to a position of local minima which tends to smooth the surface and form a compact deposit. In ballistic deposition model (left) the deposit has an open structure with many holes. However, in contrast to fractal patterns, these holes do not exist at all length scales and the resulting patterns are not fractal.

face and form a compact deposit.[20] In the absence of surface diffusion the deposit has an open structure with many holes. However, in contrast to fractal patterns, these holes do not form at all length scales and the resulting patterns are not fractal.

In the processes that we have investigated, we have found that in contrast to the structure itself which is not fractual, the surface can be described by fractal concepts. We have characterized the roughness of the surface by how widely it fluctuates from its mean value.[19] By investigating how this width varies with time in different model system we have developed a description for the fractal properties of rough surfaces. We find that surfaces must be characterized by two different fractal dimensions. One describing the variation of surface width with time (or average height) and another for describing correlations in space. Mandelbrot[1] has introduced the word *self-affine* to denote objects which need more than one fractal dimension for their description. Figure 8, shows that scaling the time dependence of the surface roughness according to our scaling description leads to the collapse of all the data into a single "universal" curve, indicating that rough surfaces are self-affine fractals. Similar plots have also been obtained for a variety of other growth processes. These show that the fractal concepts are powerful tools for describing rough surfaces.

Figure 8:

Scaling the time dependence of the surface roughness according to our theory leads to the collapse of all the data into a single curve, indicating that rough surfaces are self-affine fractals. Similar plots have also been obtained for a variety of other growth processes. These show that the fractal concepts are powerful tools for describing rough surfaces. [From ref. 19]

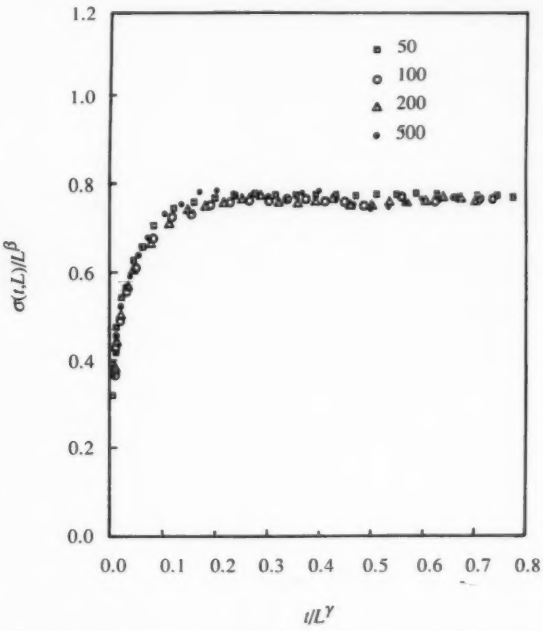

Fractal Patterns in Diffusive Growth

The formation of a wide variety of patterns is controlled by the strength of the gradient of a field at the interface between the structure and the outside.[22] For example, the rate of growth in aerosol and colloidal aggregation depends on the concentration of diffusing particles, in solidification it depends on the temperature gradient, and in dielectric breakdown it is proportional to the electric field. The common denominator among many growth processes is that the controlling fields, like temperature, concentration, pressure, and electrical potential, satisfy either the diffusion equation or the Laplace equation which is a special case of the diffusion equation. The differences in morphologies are often reflections of variations in boundary conditions and external parameters.

The most characteristic feature of diffusive growth processes is instability. The reason goes back to the fact that this type of growth is governed by the gradient of a field. As in electrostatic, the gradient of the field is largest at sharp tips or points of high curvature. Thus, when a small piece of the front gets ahead of its neighbors, it gains an advantage because the gradient at that point will become larger and this tip will have a higher probability to grow. This instability forces the boundary to break-up into dendritic arms that grow faster and faster, enventually forming a tree-like fractal pattern. In some processes such as viscous fingering [27] and dendritic solidification,[28 29] the surface tension tends to compete with this instability and prevent the patterns from becoming completely random fractals.

Figure 9:

An example of a diffusion-limited aggregation [DLA] cluster. In DLA, particles are launched from far away and allowed to diffuse. Once a diffusing particle comes in contact with a growing aggregate it sticks to it and becomes part of it. This process of releasing random walkers continues until a large cluster is formed. The simulations indicate that DLA clusters of the type shown above are fractal with a dimensionality D∼1.7 in two dimensions and D∼2.5 in three dimensions.

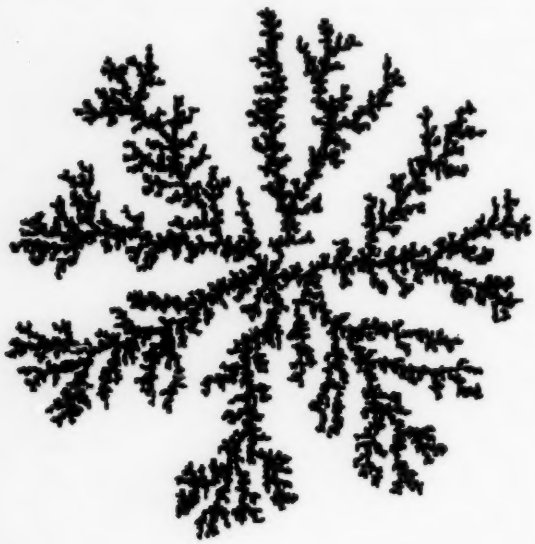

One of the consequences of the tip instability is that the mathematics of the problem is highly non-linear. In addition, it is subject to a boundary condition that is continuously moving. Therefore, progress in solving the problem of diffusive growth processes from an analytic approach has been slow. On the other hand, in recent years numerical methods have been developed that are very effective in producing a variety of the patterns that are produced by diffusion-limited or Laplacian growth processes. The most important of thse methods is the random walk simulation technique used to study diffusion-limited aggregation [DLA]. In DLA, particles are launched from far away and allowed to diffuse. Once a diffusing particle comes in contact with a growing aggregate it sticks to it and becomes part of it. This process of releasing random walkers continues until a large cluster is formed. The simulations indicate that DLA clusters (see Figure 9) are fractal with a dimensionality D∼1.7 in two dimensions and D∼2.5 in three dimensions. Due to the importance of diffusive growth processes, the random walk approach has been used extensively in solving the diffusion equation in both fractal growth [23-26] and diffusion-limited pattern formation.[27-29]

Viscous Fingering

An example of the application of DLA model for studying diffusion-limited pattern formation is shown in Figure 10. The picture on the left shows an experiment and the one on the right is the simulation [27] of a phenomenon known as viscous fingering. Viscous fingers are patterns that are formed when a less viscous fluid, such as water, pushes against a more viscous fluid, such as oil. The water, instead of pushing the oil, tunnels through it in the shape of long thin fingers, leaving much of the oil behind. This practical problem, which is of considerable interest to the oil and energy industry, is an example of pattern formation in a Laplacian field. The reason is that the pressure at the interface between the two fluids satisfies the Laplace equation. Since the DLA model solves the diffusion equation, or the Laplace equation, it can be used to simulate the formation of viscous fingers. There is however an important difference between DLA and the two-fluid problem. In viscous fingering surface tension tends to smooth out the irregularities at the interface, whereas there is no surface tension in DLA.

By incorporating surface tension and surface diffusion effects in DLA, we have effectively simulated the formation of viscous fingering patterns,[27] as shown in Figure 10. We find in agreement with the experiments, that as the surface tension is decreased the patterns become more ramified. When the two fluids are miscible, the surface tension vanishes and the resulting patterns are the same as ordinary DLA. This type of simulations and some of the recent experiments have provided new concepts and methods for investigating this complex and important problem.

Figure 10:

Simulations of viscous fingering using the diffusion-limited aggregations process. Viscous fingers are patterns that are formed when a less viscous fluid, such as water, pushes against a more viscous fluid, such as oil. The water, instead of pushing the oil, tunnels through it in the shape of long thin fingers, leaving much of the oil behind. As they grow, the fingers become narrower and narrower, until they reduce to DLA type patterns (Fig. 9). [From ref. 27]

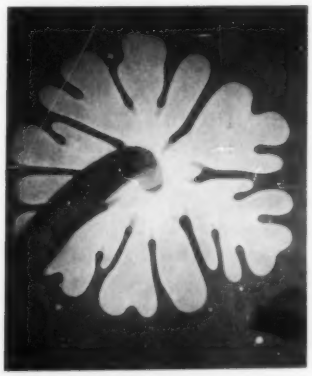

Experiment

Simulation

Laplacian Fractals

An alternative to the random walk approach is to directly solve the Laplace equation on a lattice and determine the field everywhere. The growth probability is then determined from the gradient of the field.[22] We have developed a model for studying growth in a Laplacian field which in analogy with the DLA model is based on an aggregation process.[30] However, in contrast to the DLA type models, more than one particle is added to the growing cluster in each time step. The advantage of this approach is that it reduces the random fluctuations which are inherent in the random addition of single particles in DLA-like models. In our model, the field is calculated by solving the Laplace equation on a regular lattice subject to the constraint that on the cluster the field is zero and on a large circle around the cluster the field is constant. After the field is calculated, the gradients at all the surface sites are determined. These gradients are then normalized to the maximum gradient at the surface by dividing them by the value of the largest gradient on the interface. The normalized gradient at each site is compared with a parameter p and all perimeter sites with a gradient larger than p are filled.

We first consider the case in which p is random. In the simulation,[30] the value of the normalized gradient at a perimeter site is compared with a random number and the site is occupied if the value of the gradient is larger than the random number. The process of picking a new random number for each surface site and testing and occupying the site is repeated until all the perimeter sites have been checked. A typical fractal pattern obtained from this type of simulation is shown in Figure 11. The most striking difference between Figures 9 and 11 is the highly anisotropic shape of the cluster in Figure 11. This four-fold anisotropy, which is due to the fact that the cluster was grown on a square lattice, may be used to simulate the effects of anisotropy due to crystal structure or surface tension which are present in many pattern forming processes. One of the important consequences of this anisotropy is that the fractal dimenstion of the cluster with anisotropy is smaller than the fractal dimension of an aggregate without anisotropy. Analytical[31,32] and numerical[22] studies indicate that in two dimensions the fractal dimension of an anisotropic cluster is about 1.5 rather than the value 1.7 for off-lattice DLA. This type of strong response to anisotropy is observed in many diffusion-limited phenomena, such as directional solidification and viscous fingering. It appears that anisotropy is an inherent property of many random fractal clusters.[33]

If we let p be a fixed constant, then the model becomes a *deterministic* growth process,[28] because in each growth step all perimeter sites having a normalized gradient larger than p are occupied. As a result, the patterns generated in this process are *exact* fractals, which we call *Laplace Carpets.*[28] Four examples are shown in Figure 12. In the limit $p=0$, all the perimeter sites are filled and the result is a dense polygon having the symmetry of the underlying lattice. As shown in Figure 12, for finite p, the patterns are regular fractals with a fractal dimension which decreases from 2 to 1 as p is increased from 0 to 1. The most novel feature of the Laplace carpets is that the fractal dimension in a (deterministic) Laplace growth process can be tuned continuously. Another important property of Laplace Carpets is their close similarity with cellular automaton. This is perhaps the first time that a process with long-range correlations has produced patterns similar to a process like a cellular automaton which is based on short-range, local rules.

Figure 11:

A typical fractal pattern obtained by solving the Laplace equation directly on a square lattice. The most striking difference between this cluster and the DLA pattern (Fig. 9) is the highly anisotropic shape of this cluster. This anisotropy, which is due to the fact that the cluster was grown on a square lattice, may be used to simulate the effects of anisotropy due to crystal structure or surface tension which are present in many pattern forming processes (for example, see Fig. 13). [From ref. 30]

Figure 12:

Four examples of Laplace carpets. In the limit p=0, all the perimeter sites are filled and the result is a dense polygon having the symmetry of the underlying lattice. As can be seen from these patterns, for finite p, the patterns are regular fractals with a fractal dimension which decreases from 2 to 1 as p is increased from 0 to 1.

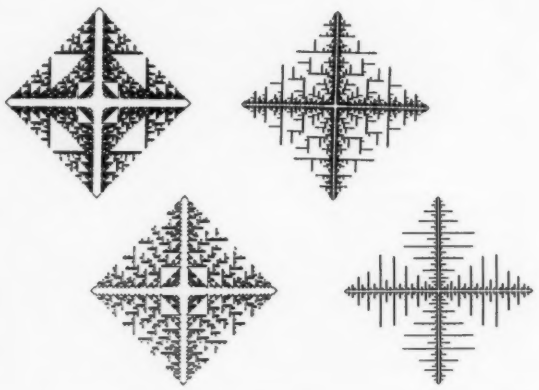

Dendritic Solidification: Snowflakes

We have extended our model for growth in a Laplacian field to simulate dendritic solidification.[28,29] The growth of dendritic crystals is one of the most profound examples of pattern formation in a diffusion-limited growth process where the temperature is the relevant field. The formation of snowflakes is perhaps the best known and puzzling example of these processes. Although subject to intensive efforts, previous methods had not produced such regular and intricate dendritic structures as are found in nature. Therefore, the development of the deterministic growth model[28] which for the first time was capable of producing realistic dendritic patterns, including snowflakes, has been an important step in developing effective methods for understanding the formation of snowflakes and dendritic crystals.

One of the key ingredients needed for the description of dendritic growth is that, by heat conservation, the normal velocity at a point on the interface is proportional to the temperature gradient. In order to implement this boundary condition it is necessary to make p a time dependent variable. We have, therefore, discretized the time interval into a piecewise function which allows us to vary p and the growth rate at the interface with time. Using this method we can produce practically all types of observed two-dimensional dendritic patterns, including snowflakes, by changing the surface tension and the growth parameters. In Figure 13, we show only a few selected examples of snowflakes generated by varying the environmental conditions during the growth. We have also investigated the fractal properties of the snowflake patterns by studying the rate of growth of the tips. We find [28] that in dendritic patterns the growth rate is similar to the growth rate in anisotropic, but random, DLA-type fractal patterns, which have a fractal dimension of about 1.5.[22 31 32] On the other hand, the dense snow crystals, such as hexagonal plates, are not fractal and have a dimension $D \sim 2$.

Figure 13:

We show only a few selected examples of snowflakes generated by varying the environmental conditions during the growth. On the left, three examples of snow crystal patterns are shown which were generated by the deterministic growth model. Three patterns of natural snowflakes are shown on the right. [From ref. 28]

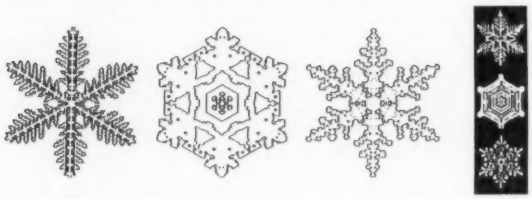

Conclusions

The wide variety of problems discussed in this brief review suggest that one of the most puzzling and challenging problems in physics is the inevitability of fractals. Fractal space and time have been found in most areas of science and technology. The advent of fractal geometry has provided scientists and engineers with fresh mathematical tools for investigating complex phenomena that had been viewed intractable by generations of scientists. In recent years, important progress has been made by applications of fractal concepts to understand a host of problems from disordered materials and complex fluids to chaos and turbulence. There is every indication, however, that despite these remarkable advances much work remains to be carried out.

Biography

Dr. Fereydoon Family is Associate Professor of Physics at Emory University. He is a Condensed Matter Theorist and has conducted research in a variety of areas from low temperature physics to polymer physics. His current interests are in the study of far from equilibrium phenomena, particular properties of random materials and surfaces and the formation of Fractal and non-Fractal patterns in growth phenomena.

References

1. B.B. Mandelbrot, *The Fractal Geometry of Nature*, (Freeman, San Francisco), 1982.

2. F. Family and D.P. Landau, Eds., *Kinetics of Aggregation and Gelation*, (North-Holland, Amsterdam), 1984.

3. S.R. Anderson and F. Family, "Percolation in an Interactive Cluster-Growth Model", *Physical Review* **A38**, 4198 (1988).

4. S.R. Anderson and F. Family, "Interactive Percolation", in *Computer Simulation Studies in Condensed Matter Physics: Recent Developments*, D.P. Landau and H.B. Schüttler (eds.), Springer Proc. Phys. (Springer-Verlag, Berlin, Heidelberg, 1988).

5. T. Vicsek and F. Family, "Dynamic Scaling for Aggregation of Clusters", *Physical Review Letters* **52**, 1669 (1984).

6. T. Vicsek and F. Family, "Critical Dynamics in Cluster-Cluster Aggregation", in *Kinetics of Aggregation and Gelation*. Eds. F. Family and D.P. Landau, (North-Holland, Amsterdam, 1984) p. 111.

7. F. family and T. Visek, "Dynamic Scaling in Aggregation Phenomena", in *Physics of Finely Divided Matter*. Edited by N. Boccara and M. Daoud (Springer-Verlag, Berlin 1985), p. 238.

8. F. Family, "Dynamics of Aggregation Phenomena", in *Proceedings of the NATO Advanced Study Institute on Growth and form*, Edited by H.E. Stanley and N. Ostrowsky (Martinus Nijhoff, Dordrecht 1985), p. 231.

9. P. Meakin, T. Vicsek and F. Family, "Dynamic Cluster-Size Distribution in Cluster-Cluster Aggregation: Effects of Cluster Diffusivity", *Physical Review* **B31**, 564 (1985).

10. T. Vicsek, P. Meakin and F. Family, "Scaling in Steady-State Cluster-Cluster Aggregation", *Physical Review* **A32**, 1122 (1985).

11. F. Family, P. Meakin and T. Vicsek, "Cluster Size Distribution in Chemically-Controlled Cluster-Cluster Aggregation", *Journal of Chemical Physics* **83**, 4144 (1985).

12. F. Family, P. Meakin and J.M. Deutch, "Kinetics of Coagulation with Fragmentation: Scaling Behavior and Fluctuations", *Physical Review Letters* **57**, 727 (1986) and **57**, 2332 (1987).

13. P. Meakin and F. Family, "Structure and Dynamics of Reaction-limited Aggregation", *Physical Review (Rapid Communications)* **A36**, 5498 (1987).

14. P. Meakin and F. Family, "Structure and Kinetics of Reaction-limited Aggregation", *Physical Review* **A38**, 2110 (1988).

15. S. Miyazima, P. Meakin and F. Family, "Aggregation of Oriented Anisotropic Particles", *Physical Review* **A36**, 1421 (1987).

16. F. Family and P. Meakin, "Scaling of the Droplet Size Distribution in Vapor-Deposited Thin Films", *Physical Review Letters* **61**, 428 (1988).

17. F. Family, "Introduction to Droplet Growth Processes: Simulations, Experiments and Theory", in Proceedings of the NATO Advanced Study Institute on *Fluctuations and Patterns*, Edited by H.E. Stanley and N. Ostrowsky (Martinus Nijhoff, Dordrecht 1988)

18. P. Meakin and F. Family, "Scaling and Growth of Droplets by Heterogeneous Nucleation", *Journal of Physics* **A21**, Lxxx (1989).

19. F. Family and T. Vicsek, "Scaling of the Active Zone in the Eden Process on Percolation Networks and the Ballistic Deposition Model", *Journal of Physics* **A18**, L75 (1985).

20. F. Family, "Scaling of Rough Surfaces: Effects of Surface Diffusion", *Journal of Physics* **A19**, L441 (1986).

21. F. Family, "Rough Surfaces: Scaling Theory and Universality", in *Universalities in Condensed Matter Physics*, R. Jullien, L. Peliti, R. Rammal and N. Boccara (eds.), Springer Proc. Phys. (Springer-Verlag, Berlin, Heidelberg, 1988).

22. F. Family, "Growth by Gradients: Fractal Growth and Pattern Formation in a Laplacian Field", in *Computer Simulation Studies in Condensed Matter Physics: Recent Developments*, D.P. Landau and H.B. Schüttler (eds.), Springer Proc. Phys. (Springer-Verlag, Berlin, Heidelberg, 1988).

23. H. Nakanishi and F. Family, "Large-Cell Monte-Carlo Renormalization of Irreversible Growth Processes", *Physical Review* **A32**, 3606 (1985) and H. Nakanishi and F. Family, "Large Cell Monte Carlo Renormalization of Growth Processes", in *Kinetics of Aggregation and Gelation*, Eds. F. Family and D.P. Landau, (North-Holland, Amsterdam, 1984) p. 79.

24. J.L. Montag, F. Family, T. Vicsek and H. Nakanishi, "An Optimized Phenomenological Renormalization Group: Applications to Diffusion-limited Aggregation", *Physical Review* **A32**, 2557 (1985).

25. P. Meakin and F. Family, "Diverging Length Scales in Diffusion limited Aggregation", *Physical Review* (Rapid Communications) **A34**, 2558 (1986).

26. D.E. Platt and F. Family, "Validity of Diffusion-Enhancement Techniques applied to Diffusion-Limited Aggregation and other Diffusive Growth Processes", *Physical Review* (Brief Reports) **A38**, 4910 (1988).

27. P. Meakin, F. Family and T. Vicsek, "Viscous Fingering Simulated by Off-lattice Aggregation", *Journal of Colloid and Interface Science* **117**, 394 (1987).

28. F. Family, D. Platt and T. Vicsek, "Deterministic Growth Model of Pattern Formation in Dendritic Solidification", *Journal of Physics* **A20**, L1177 (1987).

29. F. Family, "Mathematical Modelling of Snowflake Growth", Presented at the Symposium on the "Impact of Mathematics: Nonlinear Mathematics, Chaos, and Fractals in Science", *Proceedings of the National Academy of Sciences, Board on Mathematical Sciences* (1988).

30. F. Family, T. Vicsek and R. Taggett, "Lattice-induced Anisotropy in a Diffusion-limited Growth Model", *Journal of Physics* **A19**, L727 (1986).

31. F. Family, H.G.E. Hentschel, "Asymptotic Structure of Diffusion Limited Aggregation Clusters in Two Dimensions", *J. Chemical Society Faraday Discuss.* **83**, 139 (1987).

32. M. Matsushita, F. Family and K. Honda, "Scaling Theory for the Anisotropic Behavior of Generalized Diffusion-limited Aggregation Clusters in Two Dimensions", *Physical Review* (Rapid Communications) **A36**, 3518 (1987).

33. F. Family, T. Vicsek and P. Meakin, "Are Random Fractal Clusters Isotropic?", *Physical Review Letters* **55**, 641 (1985).

Profiles in Science

Professor Anthony J. Ferraro holds the Charles H. Fetter University Endowed Fellowship in Electrical Engineering at the Pennsylvania State University and is affiliated with the Center for Communications and Space in Sciences. As a Principal Investigator in the Office of Naval Research for many years, his research has been directed toward ionospheric modification from high-power, ground-based, high-frequency transmitting facilities. He developed the concept of radiowave phase interaction which was intended as a diagnostic technique to investigate the parameters of the lower D-region. This research led into the development of generating extremely low and very low frequency radiation by modulating the ionospheric dynamo current system by high power hf signals. This research was performed using the ionospheric heating facilities of the Arecibo, Puerto Rico and Jicamarca, Peru Observatories. Recently his research has taken him to Fairbanks, Alaska where the ONR heating facility HIPAS is located. (**HI**gh **P**ower **A**uroral **S**timulation); there he has been studying the Polar Electrojet Current System. Professor Ferraro is a Fellow of the Institute of Electrical and Electronics Engineers and a member of the International Scientific Radio Union.

OVERVIEW OF HIGH–TEMPERATURE SUPERCONDUCTIVITY:

Theory, Surfaces, Interfaces and Bulk Systems

David L. Nelson
Office of Naval Research
D. Sahu, A. Langner and Thomas F. George
State University of New York at Buffalo
J. H. Weaver and H. M. Meyer III
University of Minnesota
Aaron Wold
Brown University, Providence, Rhode Island

An overview of the theoretical and experimental aspects of the recently-discovered superconducting compounds, which resulted from research supported by The Office of Naval Research is presented. This overview is divided into three sections. In the first section a review of some of the theoretical and computational works is presented under the subsections entitled pairing mechanisms, electronic structure calculations and thermophysical properties. In the second section surface and interface chemistry issues related to the fabrication and use of high-temperature superconductors for high-performance applications are presented. Specific issues that are discussed include metallization and the formation of stable ohmic contacts, and chemically-stable overlayers that are suitable for passivation, protection and encapsulation of superconducting material structures that can then be used under a wide range of environmental conditions. Lastly, issues are discussed that are related to each of the bulk high-temperature superconducting ceramic oxides which have received so much attention the past two years. These include $Tl_2Ba_2Ca_2Cu_3O_{10}$ with a critical temperature of 125 K, which is the current record.

Theory

Since the discovery of high-temperature superconductivity in the CuO ceramics in 1986, there has been an explosion of theoretical works relating to these systems. It is not possible, in a short review of theoretical work like this, to examine the essential ideas of even a small fraction of this large body of literature. We select, quite arbitrarily, some of the work we are aware of and discuss the essential ideas of these. We apologize, in advance, to all the research workers whose work we have not reviewed.

This theoretical overview is divided into three sections: (1) pairing mechanism, (2) electronic structure calculations and finally, (3) thermophysical properties. In the section on pairing mechanism we review the basic microscopic mechanisms that might be responsible for producing superconducting states. This is a fundamental question and the success of any theoretical model addressing it should be judged in relation to the experiments it explains and the phenomena it predicts. The second part, dealing with electronic structure calculations, is quite important in that such calculations give detailed information about conduction processes, density of states and anisotropies in $\vec{k}$-space. Finally, in the section on thermophysical properties we review works relating to phonon dispersion and soft modes, dynamics of tetragonal-to-orthorhombic phase transitions and the temperature and concentration dependence of the stability of these phases.

Pairing Mechanism:

In the conventional superconductors a pair of electrons of opposite spin and momentum form a bound state which leads to a coherent and highly correlated many-body superconducting state. The attractive interaction between the electrons of the pair is mediated by lattice vibrations (phonons) and the electrons overcome their strong Coulomb repulsion by staying away from each other in time (retardation). The basic question in the new superconductors is—What is the pairing mechanism? For a review of some of the early pairing models proposed for the high-T_c materials we refer the reader to the work by Rice.[1]

One of the leading theories for the high-T_c superconductors is the resonating-valence-band (RVB) model proposed by Anderson[2] and his coworkers.[3] According to this model, the pairing mechanism is magnetic in origin and not of the conventional BCS type. The starting point of the RVB theory is a two-dimensional Hubbard model at half-filling with strong on-site Coulomb repulsion U and an attractive intersite hopping energy t. Without oxygen doping (i.e., dopant concentration $\delta = 0$), the ground state of the above model is expected to be a long-range anti-ferromagnetic (AF) state,[4] but Anderson argues that frustration might favor a RVB state over an AF ground state. The basic idea of the RVB theory is that strong electron-electron correlations result in a separation of charge degrees of freedom from spin degrees of freedom. At low doping ($\delta \neq 0$) and temperature, the quasi-particle excitations are believed to be "holons" (i.e., charge-carrying spinless particles) and "spinons" (i.e., spin-½ chargeless particles).

Superconductivity is due to formation of a condensate consisting of holon pairs. Since Bose-Einstein condensation is not possible in a strictly two-dimensional system, the interplanar couplings are important in giving rise to superconductivity.

The RVB theory has been amplified or modified in several ways,[5 6 7] the details of which we won't go into here. Rice and Wang[8] have proposed a model in which superconductivity is due to condensation of a *pair* of bosons which gives rise to quasi-particle excitation energies which are similar to those of RVB theory, but different from BCS theory. Rice and Wang, however, favor a phonon interaction which mediates the attraction between the boson pair in question. Coffey and Cox[9] have given a nice summary of the essential points of the RVB theory in Section II of their paper.

Another theory that has been proposed is the spin-bag mechanism of Schrieffer's group.[10] The starting point of their theory is the strong AF spin order in the neighborhood of the superconducting transition (T_c) and two-dimensional spin-correlations over a length L (~200 Å) in the neighborhood of the Neel transition ($T_N >> T_c$). Doping creates extra holes in the system and these are assumed to be localized over a length l ($<< L$). The spin of the hole couples to the spin density of the AF background through an exchange interaction. Within a given domain a hole produces an effective potential well or bag in its vicinity in which the hole is self-consistently trapped. The pairing is due to an effective attractive interaction between two holes which overcomes the short range Coulomb repulsion.

The importance of spins in producing a superconducting state has also been emphasized in a model proposed by Emery.[11] He has proposed that oxygen doping in the 214-material creates holes at the oxygen sites and that there is a narrow band of oxygen holes which couple strongly to the local spin configuration of the Cu-sites. This strong coupling is responsible for an attractive interaction between the oxygen holes.

We mention in passing that other mechanisms such as plasmons[12] and excitons[13] have also been proposed as possible candidates for being the condensate of the superconducting state.

Recently doubts have been expressed about the importance of the magnetic origin of the pairing interaction. The bismuth superconductors[14 15] ($BaKBiO_3$) which are closely related in structure to the earlier superconductors and which are free of copper provide counter examples[16] to the magnetic origin of superconductivity. Another counter example[16] is the 123-material in which Cu is substituted 100% by Ag bringing T_c down to 40 K. This has led some people to propose that local structure might play a role in producing a superconducting state. A recent double-well model[17] of oxygen motion indicates trends in this direction; it has been shown that a strong T-dependent electron-phonon coupling parameter could produce $T_c \approx 100$ K.

Electronic Structure Calculations:

The electronic structure[18–25] of the undoped compounds is of immense interest in getting a clue to the origin of superconductivity. These parent compounds are La_2CuO_4 (denoted by 214), $YBa_2Cu_3O_7$ (denoted by 123) and $Bi_2Sr_2CaCu_2O_8$ (denoted by 2212). The important question is: Why is the ground state of these compounds an antiferromagnetic (AF) insulator? The band structure calculations, so far performed within the local density approximation, give results which are in contrast to the experimental situation—they all produce a metallic ground state. The reason for this discrepancy is believed to be the strong electron correlations in the CuO planes which are not adequately taken into account in a band picture. It would be interesting to have electronic structure calculations which take these correlations into account. In this regard, spin-polarized band structure calculations are expected to yield improved results over conventional band structure calculations. However, the results[23–25] of spin-polarized band structure calculations do not seem to be definitive.

We would like to conclude this section by stating some of the important conclusions that have emerged from the band structure calculations. In these calculations [18, 19] the importance of the two-dimensional nature of the CuO planes was emphasized. The Copper $d(x^2-y^2)$ orbitals and the neighboring oxygen p(x,y) orbitals interact to produce bonding σ and antibonding σ^* oribtals. Similar results [20–22] were also obtained for 123- and 2212-compounds. Another important result is that the antibonding band was positioned closer to the Fermi energy E_f. In the new 2212-compounds, a pair of slightly filled Bi 6p bands provide additional carriers in the Bi-O planes.[21] A remarkable feature in these compounds is the charge separations between the two Bi-O planes.[22]

Thermophysical Properties:

In this brief discussion of the thermophysical properties of the high-T_c oxide superconductors we restrict ourselves to theoretical investigations of the lattice dynamics of these systems. In particular, we review the work on phonon modes and oxygen vacancy ordering and their influence on the structural transitions of the 214 and 123 superconductors. Knowledge of the phonon spectrum and its dependence on the oxygen distribution may prove to be of prime importance in elucidating the mechanism of high-T_c superconductivity. Several scenerios of how electron-phonon interactions can lead to high transition temperatures have been proposed including oxygen motion in double wells,[17] interlayer coupling [26, 27] and coupling to soft quasicyclic modes associated with underconstrained nearest-neighbor rearrangements.[28] At the 195th National Meeting of the American Chemical Society held at Los Angeles, California, in September 1988, three papers were presented which discussed theoretically the maximum attainable transition temperature for the copper oxide superconductors. William A. Goddard III and coworkers, on the basis of quantum-chemical calculations involving triplet magnon pairing, believe that the upper limit of the transition temperature may be as high as 230 to 250 K.[29] Daniel C. Mattis [30] predicts an upper limit of 180 K on the basis of arguments concerning the physical overlap of Wannier functions on neighboring atoms within each planar structure. R. Bruce King [31] also favors an upper limit of 180 K, basing his arguments on a graph theory analysis of the skeletal-bonding topology in the metal-oxide compounds.

There have been a limited number of theoretical investigations on phonon frequencies and eigenvectors of the $La_{2-x}(Ba, Sr)_xCuO_4$ [32–34] and $YBa_2Cu_3O_{7-\delta}$ [35–38] superconductors. Unscreened lattice dynamical models [33, 38], yielding only the bare phonon frequencies, gave fair agreement with experimentally determined total phonon density of states, mean square atomic vibrational amplitudes and Debye temperatures. Weber [32] has shown that the effect of screening, spectrum renormalization, due to conduction electrons gives rise to large Kohn anomalies near the Brillouin-zone boundary involving oxygen breathing modes. It was pointed out by Chaplot [38] that an additional effect of renormalization is to hybridize the high-frequency modes, dominated by oxygen, with the medium-frequency, heavier-nuclei modes thus making necessary an effective-mass description for the analysis of the isotope effect. Cohen, et al.[34] employing the potential-induced breathing model were able to predict the tetragonal-to-orthorhombic phase transition in La_2CuO_4 as arising from an instability, softening, in the B_{1g} tilting mode of the I4/mmm tetragonal structure. The onset of this transition has been recently derived from symmetry principles [39].

As is now well established, $YBa_2Cu_3O_{7-\delta}$ undergoes a tetragonal-to-orthorhombic phase transition for $1 > \delta > 0$ which is a consequence of oxygen vacancy ordering in the Cu-O basal plane. Several approaches have been undertaken to model this transition and describe the phase diagram in (T,δ)-space. Most treatments are of the 2-D lattice gas type, employing first and second nearest-neighbor interactions for oxygen and vacancies and solved by mean field techniques [40–48]. Another approach, which has been successful in predicting the microstructure of the multiphase region, utilizes the method of concentration waves [49]; here the oxide is treated as an interstitial compound of ordered oxygen atoms and vacancies on a simple lattice [50]. The model of Mattis [51] deserves mention since it specifically accounts for the copper-oxygen bonds and thus enables predictions to be made concerning the dielectric response of the various phases. The picture that emerges from these studies is that at high temperatures, $T > 750$ K, and/or stoichiometries $\delta < 0.5$ a tetragonal phase exists with random ordering of oxygen and vacancies in the Cu-O basal plane. For material with $\delta = 0$ the superconducting orthorhombic phase is stable with oxygen (atoms) and vacancies forming alternate chains along the crystal b-direction. At low temperatures and intermediate stoichiometries phase separation occurs with micro regions of tetragonal phase, orthorhombic phase and a second cell-doubled orthorhombic phase [48]. Phase transitions between the tetragonal and orthorhombic phases are of a second-order disorder-order type.

As a final note we mention the work on establishing the temperature domain in which thermal fluctuations and critical behavior dominate. Many of the theories described in this review are based on mean field techniques which become invalid when fluctuations are important. Estimates of the critical region, Ginzburg criterion, are in the range $\xi^G (T_c\text{-}T)/T_c \sim 0.1\text{–}0.7$ [52–54]. However, it has been pointed out that the breakdown of near-field behavior is progressive [54]; the ability of mean-field theory to predict non-universal quantities (prefactors, GL-parameters and T_c) is lost within a region $\xi^B \sim (\xi^G)^{1/2}$, Brout criterion [55], which may cover most of the superconducting regime.

Surfaces and Interfaces

The full integration of bulk and thin film high-temperature superconductors into existing and new technologies of high commercial value appears limited by a number of surface and interface materials issues. Many of these issues can be stated in general terms because they are shared by each type of ceramic superconductor (2-1-4, 1-2-3, or 2-1-2-2). Others are more specific to the material under study, e.g., the toxic character of the Tl 2-1-2-2 compound. As new materials with even higher critical temperatures are developed, analogous problems will be encountered. Hence, the knowledge base developed for one class of ceramic material may also apply to others.

First, there are issues related to materials synthesis so that structures can be fabricated with predetermined shapes, sizes, and current carrying ability. These range from macroscopic to microscopic. Second, there are challenges related to the fabrication of superconducting thin films on a variety of substrates, with Si being an obvious choice from the perspective of microelectronic devices. Third, there are issues related to the formation of stable ohmic contacts, particularly for small samples and thin films. Fourth, there are problems related to the passivation, protection or encapsulation of small structures such as fibers or thin films, so that the superconducting oxides can be used under a wide range of environments. These and a great many other issues raise challenging chemical questions. Spectacular progress has been made in the few months that the new superconductors have been in existence, and we can anticipate that rapid progress will be made in the near future. These efforts that address fundamental issues will bring us one step closer to realizing breakthroughs in technologies of high commercial value.

It might be thought that surface and interface issues should be separated from those involved in the synthesis of the superconductors themselves. This is certainly not the case, however, because many of the most exciting opportunities for these materials will be in high performance applications. In these applications, the size of the superconducting elements will be comparable to those of the other components. Scaling down or shrinking the size of a structure exacerbates problems related to interfacial phenomena. Indeed, the challenges of forming, contacting, and protecting a superconducting strip 1 μm wide and 0.1 μm thick point to the intermingling of a wide range of materials issues.

To date, issues related to bulk synthesis and surface or interface characterization have also been intimately tied. This can be seen by noting that the starting point for surface or interface research is a well-characterized bulk material. Unfortunately for the surface scientist, early samples did not spring completely characterized from the firing furnaces, to paraphrase the springing-forth of Minerva completely armed from the head of Jupiter. Instead, early samples were sintered, were 70-90% dense, and individual grains were clad with other phases[56,57]. Difficulties in characterizing these interfaces and identifying their intrinsic properties are reflected in the literature of the last year for the 1-2-3 and 2-1-4 materials, and the last few months for the 2-1-2-2 materials. Only recently have bulk samples of sufficient quality been available so that fracturing could provide a clean surface[56]. Today, it is relatively routine to find single crystals having dimensions of greater than 1 mm, and several small companies are preparing to sell single crystals as large a 1 cm x 1 cm so that full characterization can be achieved.

Early studies indicated that polycrystalline, sintered samples of the 1-2-3 and 2-1-4 materials degraded rapidly upon exposure to a range of environments, including H_2O, CO, CO_2, O_2 and solvents.[58-60] More recent work suggests that degradation is much slower and that some of the early problems were related to the intergranular phases (e.g. carbonates or cuprates). Early work also showed that exposure of the 1-2-3's to high-intensity ultraviolet and X-ray photon beams produces substantial changes in the surfaces.[61] Again, recent work has indicated that most of the changes are related to the presence of second phases and were not intrinsic to the superconductors. At the same time, studies by Rosenberg and coworker[62] pointed out some of the details of photon stimulated desorption. Electron beams of high current or high energy also induce damage. Exposure of these materials to energetic ions, such as used in Ar sputtering, leads to surface modification, structural changes, and the loss of superconductivity.[56] This damage points to the fragile character of these superconductors but also indicates that it may be possible to selectively alter portions of a thin film, for example writing nonsuperconducting lines on a superconducting template.

An issue that has arisen repeatedly has been the possibility of oxygen loss through the surface at room temperature. To our knowledge, there is no clear evidence that oxygen is lost under static vacuum conditions. Instead, the exposure of freshly prepared surfaces to ultrahigh vacuum leads to the chemisorption of residual gases from the vacuum system. Recent work with single crystals has provided evidence for the rearrangement of surface atoms after cleaving in vacuum.[63] This has been attributed to transgranular fracture and the exposure of energetically unfavorable surfaces. Indeed, such effects can be understood in terms of the highly anisotropic unit cell, but the restructuring does not necessarily result in oxygen loss.

Attempts to form contacts to surfaces or to investigate the electrical properties of the high-temperature superconductors have often been complicated by nonreproducibility. This can be related to the chemical processes that occur at these surfaces. As detailed studies of representative interfaces have shown, there is a strong tendency for reactive metals to leach oxygen from the superconductor to form new metal oxide bonding configurations.[56,64] The result of this interfacial chemistry is a heterogeneous transition region between the buried superconductor and the metal film. In particular, a cross section through an interface based on the 1-2-3, 2-1-4 or 2-1-2-2 superconductors would show the superconductor; a region where oxygen has been removed,

where the structure is likely to be disrupted, and which is not superconducting; a region where the metal adatoms have formed electrically-resistive oxides; and the metal overlayer, possibly containing oxygen and dissociated superconductor atoms in solution and at the surface. Such an interface is shown schematically in Fig. 1. These interfaces are metastable because thermal processing will enhance oxygen transport to the metal layer and will increase the amount of substrate disruption. Certainly, these interfaces would not form the ohmic contacts desired in device applications. Likewise, the cladding of superconducting filaments with copper sheaths does not seem propitious since there will be interfacial interactions and the formation of a nonsuperconducting layer. The scale of this disrupted region is at least 50 Å for room temperature metal deposition and is likely to be much larger if the interface is processed at a higher temperature.

Ohmic contacts to these superconductors can be formed with Ag and Au overlayers.[65] These metals show minimal tendency to form oxides, and their deposition does not seriously disrupt the superconductor. For contracts, then, these metals appear to be the materials of choice. Two caveats should be noted, however. First, processing may lead to Au clustering, as has been observed for Au layers on many substrates. Second, if the surface to be metallized has been exposed to the air, it will be coated with hydrocarbons, water vapor and the like, and its superconducting properties will most likely be compromised. Attempts using Ar-ion sputtering to remove these contaminants prior to metallization have been successful, but almost certainly at the expense of the structural integrity of the surface. It remains to be seen whether the amount of surface damage (and loss of superconductivity) compromises the effective use of this approach to the fabrication of ohmic contacts for devices.

The protection of these superconductors is also crucial if they are to be integrated with other technologies. Much less is known about such passivation issues, although attempts are presently under way to develop protective overlayers. Two types of materials that have been examined so far and appear promising are metal oxides and non-metallic insulators.[66] Metal oxides have been formed by the deposition of metal atoms in an activated oxygen atmosphere to form a metal oxide precursor that does not leach oxygen from the substrate. The oxide layer then serves as a diffusion barrier against oxygen loss or atomic intermixing. To date, efforts have been successful with the oxides of Al and Bi, and it is likely that other oxides will prove to be effective as passivation layers and/or diffusion barriers. Those investigated so far are insulators, but future work may lead to conducting oxides that can serve as both contacts and passivators.

The second type of material that shows promise for passivation and electrical isolation is CaF_2.[66] This large-bandgap ionic insulator has a high static dielectric constant, can be readily evaporated from thermal sources in molecular form, and shows no tendency to modify the superconductor. As such, it may be useful as a dielectric layer in advanced devices.

We also note that both organic and inorganic polymers may be useful as encapsulants. In fact, fully protective coatings for high temperature superconductors may need to be developed to meet the specific demands of large- and small-scale applications. These protective coatings will likely involve a multilayer structure that would consist of thin- or thick-films of metals, low dielectric ceramics, and possibly organic and inorganic polymeric films. These multifunctional coatings would be effective as a diffusion barrier, would withstand environmental stress and temperature cycling, and would maintain strong adhesion. Specific opportunities exist for the synthesis of precursor molecules, such as organometallics, for chemical vapor deposition (CVD), or sol/gel approaches for low temperature fabrication of these multilayer protective coatings.

Bulk Superconducting Ceramic Oxides

Superconducting oxides have been known since 1964, but until recently the intermetallic compounds showed higher superconducting temperatures. In 1975 research scientists at E. I. DuPont de Nemours[67] discovered superconductivity in the system $BaPb_{1-x}Bi_xO_3$ with a T_c of 13 K. The structure for the superconducting composition in this system is only slightly distorted from the ideal cubic perovskite structure. It is generally accepted that a disproportionation of the Bi(IV) occurs, namely, $2Bi(IV)\ (6s^1) \rightarrow Bi(III)\ (6s^2) + Bi(V)(6s^0)$ at approximately 30 percent Bi. Sleight found that the best superconductors were single phase prepared by quenching from a rather restricted single-phase region, and hence these phases are actually metastable materials. At equilibrium conditions, two phases with different values of x would exist; the phase with a lower value of x would be metallic and with a higher value of x would be a semiconductor. It is important to keep in mind that the actual assignment of formal valence states is a convenient way of electron accounting; the actual states include appreciable admixing of anion functions. The system $BaPb_{1-x}Bi_XO_3$ should be studied further since it contains compositions showing the highest T_c for any superconductor not containing a transition element. Recently, for example, Cava and Batlogg[14] have shown that $Ba_6K_4\ BiO_3$ gave a T_c of almost 30 K, which is considerably higher than the 13 K reported for $BaPb_{75}\ 75Bi_{25}\ O_3$.

La_2CuO_4 was reported by Longo and Raccah[68] to show an orthorhombic distortion of the K_2NiF_4 structure with a=5.363 Å, b=5.409 Å and c=13.17 Å. It was also reported[69,70] that La_2CuO_4 has a variable concentration of anion vacancies which may be represented as La_2CuO_{2-x}.

Superconductivity has been reported for some preparations of La_2CuO_4. However, there appears to be some question as to the stoichiometry of these products since only a small portion of the material seems to exhibit superconductivity.[71]

The extent of the anion vacancies has been recently re-examined,[72] and the magnitude of this deficiency is less than can be unambiguously ascertained by direct thermogravimetric analysis which has a limit of accuracy in x of 0.01 for the composition La_2CuO_{4-x}. However, significant shifts in the Néel temperatures confirm a small variation in anion vacancy concentrations.

In the $La_{2-x}A_xCuO_4$ phases (A=Ca,Sr,Ba) the substitution of the alkaline earth cation for the rare earth depresses the tetragonal-to-orthorhombic transition temperature. The transition disappears completely at x> 0.2, which is about the composition for which superconductivity is no longer observed. Compositions of $La_{2-x}A_xCuO_4$ can also be prepared[73, 74] where A is Cd(II) or Pb(II). However, these phases are not superconducting, and it appears that the more basic divalent cations are necessary to allow Cu(III) to coexist with O^{2-}. The existence of Cu(I) and Cu(III) in $La_{1.8}Sr_{.2}CuO_4$ is consistent with the ESR spectra, which shows the absence of square planar Cu(II), and the Pauli-paramagnetic behavior over the temperature range from 77 to 300 K. Since the Pauli-paramagnetic behavior of $La_{1.8}Sr_2CuO_4$ is consistent with delocalized electrons, this would also indicate a high probability for the existence of Cu(I)–Cu(III) formed as a result of disproportionation of Cu(II).[75] Subramanian et al.[76] have recently substituted both sodium and potassium into La_2CuO_4, giving rise to the compositions $La_{2-x}A_xCuO_4$ (A = Na,K). However, only the sodium substituted samples exhibited superconducting behavior.

The compound $Ba_2YCu_3O_7$ shows a superconducting transition of ~93 K and crystallizes as a defect perovskite. The unit cell of $Ba_2YCu_3O_7$ is orthorhombic (Pmmm) with a=3.8198(1) Å, b=3.8849(1) Å and c=11.6762(3) Å. The structure may be considered as an oxygen-deficient perovskite with tripled unit cells due to Ba-Y ordering along the c-axis. For $Ba_2YCu_3O_7$, the oxygens occupy 7/9 of the anion sites. One third of the copper is in 4-fold coordination and 2/3 are five-fold coordinated. A reversible structural transformation occurs with changing oxygen stoichiometry going from orthorhombic at x=7.0 to tetragonal at x=6.0.[77] The value x = 7.0 is achieved by annealing in oxygen at 400–500°C, and this composition shows the sharpest superconducting transition. It was shown by Davison et al.[75] that these materials are readily attacked by water and carbon dioxide in air to produce carbonates.

Recently Maeda et al.[78] reported that a superconducting transition of 120 K was obtained in the Bi/Sr/Ca/Cu/O system. The structure was determined for the composition $Bi_2Sr_2CaCu_2O_8$ by several laboratories.[79–81]

In most of the studies reported to date on the Bi/Sr/Cu/O system measurements were made on single crystals selected from multiphase products. The group at DuPont selected platy crystals having the composition $Bi_2Sr_{3-x}Ca_xCu_2O_{8+y}$ (0.9>x>0.4) which showed a T_c~95 K. Crystals of $Bi_2Sr_{3-x}Ca_xCu_2O_{8\pm y}$ for x=0.5 gave orthorhombic cell constants a =5.399 Å, b=5.414 Å, c=30.904 Å.[79] These cell dimensions are consistent with the results of other investigators[80 81]. The structure consists of pairs of CuO_2 sheets interleaved by Ca(Sr), alternating with double bismuthoxide layers. Sunshine et al.[81] have indicated that the addition of Pb to this system raises the T_c above 100 K. There are now three groups of superconducting oxides which contain the mixed Cu(II)-Cu(III) oxidation states, namely $La_{2-x}A^{II}CuO_4$ where A^{II}=Ba,Sr,Ca; $RBa_2Cu_3O_7$ where R is almost any lanthanide; and $Bi_2Sr_{3-x}Ca_xCu_2O_{8+y}$.

Sheng and Herman have recently reported[82] on a high-temperature superconducting phase in the system Tl/Ba/Ca/Cu/O. Two phases were identified by Hazen et al.[83], namely $Tl/Ba/CaCu_2O_9$ and $Tl_2Ba_2Ca_2Cu_3O_{10}$. Sleight et al.[79 84] have also reported on the structure of $Tl_2Ba_2CaCu_2O_8$ as well as $Tl_2Ba_2CuO_6$. In addition, the superconductor $Tl_2Ba_2Ca_2Cu_3O_{10}$ has been prepared by the DuPont group[85] and shows the highest T_c of any known bulk superconductor, namely ~125 K.

A series of oxides with high T_c values has now been studied for the type $(A^{III}O)_2A_2^{II}Ca_{n-1}Cu_nO_{2.2n}$ where A(III) is Bi or Tl, A(II) is Ba or Sr, and n is the number of Cu-O sheets stacked. To date, n=3 is the maximum number of stacked Cu-O sheets examined consecutively. There appears to be a general trend whereby T_c increases as n increases. Unfortunately, these phases involve rather complex ordering, crystals of the phases are grown in sealed gold tubes, and excess reactants are always present. The toxicity as well as volatility of thallium, coupled with problems in obtaining reasonable quantities of homogeneous single-phase material, presents a challenge to the synthetic chemist. It will also be interesting to see if these materials are truly more stable over time than the $La_{2-x}A_xCuO_4$ or $RBa_2Cu_3O_7$ phases.

When superconductivity in oxides was first discovered in 1964, it created little excitement because the T_c's were lower than those found for intermetallic compounds. However, today there exists a number of oxides having metal-oxygen σ^* bands[86 87] which give the highest T_c values of all known superconductors. Despite optimistic reports from numerous laboratories, a number of fundamental chemical problems exist which make commercialization of these oxides particularly challenging. The following is a brief summary of these difficulties.

The best superconductors in the $BaPb_{1-x}Bi_xO_3$ system are metastable materials prepared by quenching from elevated temperatures. These compounds become two-phase if they are annealed at lower temperatures. In fact, even in the single-phase high-T_c region there will be a tendency for Pb and Bi segregation on a short-range basis. This is probably why it is difficult to obtain sharp transistions in this system, regardless of the value of x.

The compounds which crystallize with the K_2NiF_4 structure (La_2CuO_4, etc.) also have serious chemical problems associated with them. The compound La_2CuO_4 can be non-stoichiometric in several different ways. Most of the at-

tention has emphasized the oxygen stoichiometry, i.e., La_2CuO_{4-x}. There is a tendency to form intergrowth phases [88] of the type $La_2CuO_4nLaCuO_3$, i.e., perovskite $LaCuO_3$ intergrowth with K_2NiF_4-type La_2CuO_4.

For all of the copper-containing superconductors where copper is found to be present with a formal valence of Cu(III), we are actually dealing with the reactivity of holes located in the π^* band [86 87]. This results in instability of these copper compounds when exposed to moisture and/or air. It is highly unlikely that treating the surface of such bulk compounds with a protective coating will do much to prevent their destruction under most operating conditions. The high mobility of copper in ternary oxides, even at room temperature, will add to the reactivity of superconductor surfaces with air and moisture. Furthermore, non-superconducting phases can readily form with stoichiometries close to those of the superconducting phases. Hence, pure superconducting materials with the necessary properties will be difficult to prepare.

Single crystal growth can be achieved from melts of many of the complex superconducting copper oxides. However, many are found to melt incongruently, as well as to form intergrowths of nonsuperconducting phases. Twinning and poor crystal growth are the rule rather than the exception.

References

1. Rice, T.M. *Z. Phys. B* 1987, *67*, 141.

2. Anderson, P.W. *Mater. Res. Bull.* 1973, *8*, 153; Fazekas, P.; Anderson, P.W. *Phil. Mag.* 1974, *30*, 432 Anderson, P.W., *Science*, 1987, *235*, 1196.

3. Baskaran, G.; Zou, Z.; Anderson, P.W. *Solid State Commun.* 1987, *63*, 973; Anderson, P.W.; Baskaran, G.; Zou, Z.; Hsu, T.C. *Phys. Rev. Lett.* 1987, *58*, 2790; Anderson, P.W.; Zou, Z. *Phys. Rev. Lett.* 1988, *60*, 132; Wheatly, J.M.; Hsu, T.C.; Anderson, P.W. *Phys. Rev. B* 1988, *37*, 5897.

4. Hirsch, J.E. *Phys. Rev. B* 1985, *31*, 4403.

5. Kivelson, S.A.; Rokhsar, D.S.; Sethna, J.P. *Phys. Rev. B*, 1987, *35*, 857.

6. Ruckenstein, A.E., Hirschfeld, P.J.; Appel, J. *Phys. Rev. B.* 1987, *36*, 857.

7. Kotliar, G. *Phys. Rev. B* 1988, *37*, 3664.

8. Rice, M.J.; Wang, Y.R. *Phys. Rev. B*, 1988, *37*, 5893.

9. Coffey, L.; Cox, D.L. *Phys. Rev. B*, 1988, *37*, 3389.

10. Schrieffer, J.R.; Wen, X.-G.; Zhang. S.-C. *Phys. Rev. Lett.* 1988, *60*, 944.

11. Emery, V., *Phy. Rev. Lett.* 1987, *58*, 2794.

12. Varma, C.M.; Schmitt-Rink, S; Abrahams, E. *Solid State Commun.* 1987, *62*, 681.

13. Ruvalds, J. *Phys. Rev. B* 1987, *36*, 8869.

14. Cava, R.J.; Batlogg, A.B. *Nature* 1988, *332*, 814.

15. Rice, T.M. *Nature* 1988, *332*, 780.

16. Kao, Y.H. colloquium talk at SUNY-Buffalo on May 24, 1988.

17. Hardy, J.R.; Flochen, J.W. *Phys. Rev. Lett.* 1988, *60*, 2191.

18. Mattheiss, L.F. *Phys. Rev. Lett.* 1987, *58*, 1028.

19. Yu, J.; Freeman, A.J.; Xu, J.-H. *Phys. Rev. Lett.* 1987, *58*, 1035.

20. Mattheiss, L.F.; Hamann, D.R. *Solid State Commun.* 1987, *63*, 395.

21. Hybersten, M.S.; Mattheiss, L.F. *Phys. Rev. Lett.* 1988, *60*, 1661.

22. Krakauer, H.; Pickett, W.E. *Phys. Rev. Lett.* 1988, *60*, 1665.

23. Guo. G.Y.; Temmerman, W.; Stocks, G. *J. Phys. C.* 1988, *21*, L103.

24. Leung, T.C.; Wang, X.W.; Harmon, B.N. *Phys. Rev. B* 1988, *37*, 384.

25. Sterne, P.A.; Wang, C.S. *Phys. Rev. B* 1988, *37*, 7472.

26. Arnold, G.B. In *Novel Superconductivity*; Kresin, V.Z.; Wolf, S.A., Eds.; Plenum: New York, 1987; p. 323.

27. Gulasci, Zs.; Gulasci, M.; Pop, I. *Phys. Rev. B* 1988, *37*, 2247.

28. Phillips, J.C. *Phys. Rev. Lett.* 1987, *59*, 1856.

29. C & EN *66*, 6 (1988).

30. D.C. Mattis in *Chemistry of High-Temperature Supercodncutors II*, ed. by D.L. Nelson and T.F. George (American Chemical Society, Washington, D.C.) ACHS Symp. Ser. *377*, 103 (1988).

31. R.B. King, in *Chemistry of High-Temperature Superconductors II*, ed. by D.L. Nelson and T.F. George (American Chemical Society, Washington, D.C.) ACS Symp. Ser. *377*, 54 (1988).

32. Weber, W. *Phys. Rev. Lett.* 1987, *58*, 1371; 1987, *58*, 2154(E).

33. Prade, J.; Kulkarni, A.D.; de Wette, F.W.; Kress, W.; Cardona, M.; Reiger, R.; Schröder, U. *Solid State Commun.* 1987, *64*, 1267.

34. Cohen, R.E.; Pickett, W.E.; Boyer, L.L.; Krakauer, H. *Phys. Rev. Lett.* 1988, *60*, 817.

35. Thomsen, C.; Cardona, M.; Kress, W.; Liu, R.; Genzel, L.; Bauer, M.; Schönhers, E.; Schröder, U. *Solid State Commun.* 1987, *65*, 1139.

36. Bates, F.E.; Eldridge, J.E. *Solid State Commun.* 1987, *64*, 1435.

37. Liu, R.; Thomsen, C.; Kress, W.; Cardona, M.; Gegenheimer, B.; de Wette, F.W.; Prade, J.; Kulkarni, A.D.; Schröder, U. *Phys. Rev. B* 1988, *37*, 7971.

38. Chaplot, S.L. *Phys. Rev. B* 1988, *37*, 7435.

39. Sahu, D.; George, T.F. *Solid State Commun.* 1988, *65*, 1371.

40. Bakker, H.; Welch, D.; Lazareth, O. *Solid State Commun.* 1987, *64*, 237.

41. Shi-jie, X. *J. Phys.* 1988, *C21*, L69.

42. Kubo, Y.; Igarashi, H. *Jpn. J. Appl. Phys.* 1987, *26*, L1988.

43. Inouie, M.; Takemori, T.; Sakudo, T. *Jpn. J. Appl. Phys.* 1987, *26*, L2015.

44. Bell, J.M. *Phys. Rev. B* 1988, *37*, 541.

45. Varea, C.; Robledo, A. *Mod. Phys. Lett. B* 1988, *1*, in press.

46. Sanchez, J.M.; Mejia-Lia, F.; Moran-Lopez, J.L. *Phys. Rev. B* 1988, *37*, 3678.

47. Khachaturyan, A.G.; Semenovskaya, S.V.; Morris, Jr., J.W. *Phys. Rev. B*, 1988, *37*, 2243.

48. Wille, L.T.; Berera, A.; de Fontaine, D. *Phys. Rev. Lett.* 1988, *60*, 1065.

49. Khachaturyan, A.G.; Morris, Jr., J.W. *Phys. Rev. Lett.* 1987, *59*, 2776.

50. Pokrovskii, B.I.; Khachaturyan, A.G. *J. Solid State Chem.* 1986, *61*, 137, 154.

51. Mattis, D.C. *Int. J. Mod. Phys. Lett.*, in press.

52. Deutscher, G. In *Novel Superconductivity*; Kresin, V.Z.; Wolf, S.A., Eds.; Plenum: New York, 1987; p. 293.

53. Lobb, C.J. *Phys. Rev. B* 1987, *36*, 3930.

54. Kapitulnik, A.; Beasley, M.R.; Castellani, C.; DiCastro, C. *Phys. Rev. B* 1988, *37*, 537.

55. Hohenberg, P.C. In *Proceedings of Fluctuations in Superconductors*; Goree, W.S.; Chilton, F., Eds.; Stanford Research Institute, Stanford, 1968.

56. Meyer, H.M.; Wagener, T.J.; Hill, D.M.; Gao, Y.; Weaver, J.H.; Capone, D.W.; Goretta, K.C. *Phys. Rev. B* 1988, 38, xxx.

57. Verhoven, J.D.; Bevolo, A.J.; McCullum, R.W.; Gibson, E.D.; Noack, M.A. *Appl. Phys. Lett.* 1987, *52*, 745.

58. Yan, M.F.; Barnes, R.L.; O'Bryan, Jr., H.M.; Gallagher, P.K.; Sherwood, P.K.; Jim, S. *Appl. Phys. Lett.* 1987, *51*, 532.

59. Qui, S.L.; Ruckman, M.W.; Brookes, N.B.; Johnson, P.D.; Chen, J.; Lin, C.L.; Strongin, M.; Sinkovic, B.; Crow, J.E.; Jee, Chou-Soo *Phys. Rev. B* 1988, *37*, 3747.

60. Kurtz, R.L.; Stockbauer, R.A.; Madey, T.E.; Mueller, D.; Shih, A.; Toth, L. *Phys. Rev. B* 1988, *37*, 7936.

61. Chang, Y.; Onellion, M.; Niles, D.W.; Margaritondo, G. *Phys. Rev. B* 1987, *36*, 3986.

62. Rosenberg, R.A.; Wen, C.-R. *Phys. Rev. B* 1988, *37*, 5841.

63. Weaver, J.H.; Meyer, H.M.; Wagener, T.J.; Hill, D.M.; Peterson, D.; Fisk, Z.; Arko, A.J. *Phys. Rev. B* (submitted).

64. Gao, Y.; Wagener, T.J.; Hill, D.M.; Meyer, H.M.; Weaver, J.H.; Arko, A.J.; Flandermeyer, B.; Capone, D.W. In *Chemistry of High-Temperature Superconductors*; American Chemical Society Symposium Series 351, Nelson, D.L.; Whittingham, M. Stanley; George, T.F., Eds.; Washington, D.C., 1987, p. 212; Gao, Y.; Meyer, H.M.; Wagener, T.J.; Hill, D.M.; Anderson, S.G.; Weaver, J.H.; Flandermeyer, B.; Capone, D.W. In *Thin Film Processing and Characterization of High-Temperature Superconductors*; American Institute of Physics Conference Proceedings No. 165, Harper, J.M.E.; Colton, R.J.; Feldman, L.C.; Eds.; New York, NY, 1987; p. 358.

65. Wagener, T.J.; Vitomirov, I.M.; Aldao, C.M.; Joyce, J.J.; Capasso, C.; Weaver, J.H.; Capone, D.W. *Phys. Rev. B* 1988, *38*, xxx; Meyer, H.M.; Wagener, T.J.; Hill, D.M.; Gao, Y.; Anderson, S.G.; Krhan, S.D.; Weaver, J.H.; Flandermeyer, B.; Capone, D.W. *Appl. Phys. Lett.* 1987, *51*, 1118.

66. See the chapter in this book by Meyer et al.

67. Sleight, A.W.; Gillson, J.L.; Bierstedt, P.E. *Solid State Commun.* 1975, *17*, 299.

68. Longo, J.M.; Raccah, P.J. *J. Solid State Chem.* 1973, *6*, 526.

69. Johnston, D.C.; Stokes, J.P.; Goshorn, D.P.; Lewandowski, J.T. *Phys. Rev. B* 1987, *36*, 4007.

70. Mitsuda, S.; Shirane, G.; Sinha, S.K.; Johnston, D.C.; Alvarez, M.S.; Vaknin, D.; Moncton, D.E. *Phys. Rev. B*, 1987, *36*, 822.

71. Grant, P.M.; Parkin, S.S.P.; Lee, V.Y.; Engler, E.M.; Ramirez, M.L.; Vazquez, J.E.; Lim, G.; Jacowitz, R.D.; Green, R.L. *Phys. Rev. Lett.* 1987, *58*, 2482.

72. DiCarlo, J.; Niu, C.M.; Dwight, K.; Wold, A. (see this volume).

73. Shaplygin, I.S.; Kakhan, B.G.; Lazareo, Russ. V.B. *J. Inorg. Chem.* 1979, *24*, 820.

74. Gopalaknshnan, J.; Subramanian, M.A.; Sleight, A.W. In *Superconducting: Synthesis, Properties and Processing*; Hatfield, W., Ed.; Marcel Dekker: New York, 1988.

75. Davison, S.; Smith, K.; Zhang, Y.-C.; Liu, J-H.; Kershaw, R.; Dwight, K.; Reiger, P.H.; Wold, A. *ACS Symposium Series No. 351*, 1987, 65.

76. Subramanian, M.A.; Gopalaknshnan, J.; Torardi, C.C. Askew, T.R.; Flippen, R.B.; Sleight, A.W. *Science*, 1988, *240*, 495.

77. Gallagher, P.K.; O'Bryan, H.M.; Sunshine, S.A.; Murphy, D.W. *Mat. Res. Bull.* 1987, *22*, 995.

78. Maeda, H.; Tanaka, Y.; Fukutomi, M.; and Asano, T. *Jpn. J. Appl. Phys.* 1988, *27*, L209.

79. Subramanian, M.A.; Torardi, C.C.; Calabrese, J.C.; Gopalaknshnan, J.; Morrissey, K.J.; Askew, J.R.; Flippen, R.B.; Chowdry, U.; Sleight, A.W. *Science* 1988, *239*, 1015.

80. Tarascon, J.M.; LaPage, Y.; Barboux, P.; Bagley, B.G.; Greene, L.H.; McKinnon, W.R.; Hull, G.W.; Giroud, M.; Hwang, D.M. *Phys. Rev. B*, December 1988, 38.

81. Sunshine, S.A.; Siegrist, T.; Schneemeyer, L.F.; Murphy, D.W.; Cava, R.J.; Batloggg, B.; van Dover, R.B.; Fleming, R.M.; Olanim, S.H.; Nakahara, S.; Farrow, R.; Krajewski, J.J.; Zahurak, S.M.; Wasczak, J.V.; Marshall, J.H.; Marsh, P.; Rupp, Jr., L.W.; Peck, W.F. *Phys. Rev. B* 1988, *38*, 893.

82. Sheng, Z.Z.; Hermann, A.M. *Nature* 1988, *332*, 55; 1988, *332*, 138.

83. Hazen, R.M.; Finger, L.W.; Angel, R.J.; Prewitt, C.T.; Ross, N.L.; Hadidiacos, C.G.; Heaney, P.J.; Veblen, D.R.; Sheng, Z.Z.; El Ali, A.; Hermann, A.M. *Phys. Rev. Lett.* 1988, *60*, 1657.

84. Torardi, C.C.; Subramanian, M.A.; Calabrese, J.C.; Gopalaknshnan, J.; McCarron, E.M.; Morrissey, K.J.; Askew, T.R.; Flippen, R.B.; Chowdry, U.; Sleight, A.W. *Phys. Rev. B* 1988, *38*, 225.

85. Torardi, C.C.; Subramanian, M.A. Calbabrese; Gopalaknshnan, J.; Morrissey, K.J.; Askew, T.R.; Flippen, R.P.; Chowdry, U.; Sleight, A.W. *Science* 1988, *240*, 631.

86. Davies, A.H.; Tilley, R.J.D. *Nature* 1987, *326*, 859.

87. Goodenough, J.B. *J. Mat. Ed.* 1987, *9*, 619.

88. Goodenough, J.B.; Manthiram, A.; Dai, Y.; Campion, A. *Superconductor Science and Technology*, in press.

Biographies

Dr. David Nelson is the program manager in the Physical and Solid State Chemistry Division of the Office of Naval Research. His papers and research have been mainly in the field of fluid/solid surface interactions and high-temperature superconductors. Recently he edited with T. F. George, "Chemistry of High-Temperature Superconductors" for the American Chemical Society. He is a member of the American Chemical Society and the Electrochemical Society.

Dr. D. Sahu is a research associate in the Department of Physics at the State University of New York (SUNY) at Buffalo. His research and publications are mainly in the areas of phase transitions and condensed matter, ultra fast processes, and resonant tunneling diodes.

Dr. A. Langner is a research associate in the Department of Physics at SUNY at Buffalo. Chemical engineering and polymer chemistry are his major research areas.

Dr. Thomas George is the Dean of Natural Sciences and Mathematics, SUNY at Buffalo, as well as Professor of Chemistry. For many years he has been a principle investigator for the Office of Naval Research. His major research interest and publications are in the field of the interaction of lasers with solid surfaces.

Dr. J. H. Weaver is Professor of Chemical Engineering and Materials Science at the University of Minnesota. Professor Weaver's research and papers have been mainly in the area of physics and chemistry interfaces. Dr. Meyer is a Research Associate in Professor Weaver's department.

Dr. Aaron Wold is the Vernon K. Krieble Professor of Chemistry at Brown University. His publications and research have been primarily in the fields of transition metal compounds, of new superconductors, synthesis of materials which transmit in the infrared, and development of new techniques for the preparation of thin films.

ONR Leads in Optimization

Neal Glassman
Office of Naval Research

In October 1986, the Office of Naval Research undertook an accelerated research initiative in projective transformations for optimization. The initiative was motivated by the startling announcement by Narendra Karmarkar and Bell Laboratories in the fall of 1984 of a new algorithm for linear programming.

The new initiative exemplifies the response to the challenging and urgent optimization problems found throughout the Navy, with its complex multi-echelon inventory systems, the world's largest warehouses, industral-type job shops, daily multi-criterion manpower assignment problems, engineering design applications, and strategic and tactical planning and allocation decisions of the greatest importance. During the last three decades, through ONR, the Navy has been investing in and developing the mathematics of optimization as well as specialized algorithms, codes, and applications.

ONR supports optimization principally through its mathematics division. Although several individual programs within the division contribute to the effort, numerical analysis and discrete mathematics in particular, the focus for optimization is in the operations research program.

The new algorithm, by Karmarkar's account, yielded running times for some problems that were hundreds of times faster than those of the simplex method. In addition to this astounding computational performance, the algorithm was significant in two respects. First, it reached an optimal solution in a number of iterations that is a polynomial function of problem size. Second, it operated in the interior of the linear programming (LP)-polytope. A polytope is the higher dimensional analog of a polygon, which represents the set of all feasible points. All of these attributes contributed to the widespread enthusiasm that greeted Karmarkar's announcement.

The simplex method of the solution of linear programming problems operates on the surface of the LP-polytope. The algorithm moves from vertex to vertex until it finds a vertex where the objective function is optimal. Roughly speaking, the complexity of the network of edges and vertices that defines the surface of the polytope grows exponentially with the size of the problem. For this reason, the simplex method is an exponential algorithm: in the worst case, the number of iterations required to reach an optimal vertex is an exponential function of the number of variables and constraints. The insight that an algorithm operating in the interior of the polytope might avoid such complexity is not new. In fact, since the invention of the simplex method in the mid-1940's, hundreds of papers implementing this idea have been written. None, however, was successful in yielding faster running times on problems of interest.

Khachian's algorithm, one such interior method, was announced in 1978. The first algorithm for linear programming with a polynomial performance bound, it verified the correctness of the insight that an interior method could avoid much of the complexity associated with the simplex method. Despite its theoretical superiority for worst-case problems, Khachian's algorithm proved to be impractically slow on real-world problems. The difficulty with it and the other previously developed interior methods lies in finding the direction toward the optimum from an arbitrary interior point. LP-polytopes derived from large real-world problems tend to be long and narrow, like carrot sticks, not shaped like a cube. For this reason, it is very difficult to find an interior point near the center and even more difficult to find a direction that does not quickly hit the boundary. Karmarkar's contribution was the discovery that the application of a suitable transformation, a projective transformation, to the n-dimensional space and to a specified interior point produces a new problem with desirable properties in a transformed space. In the transformed space, the specified interior point is near the center of gravity of the polytope. From this point, a direction can easily be determined that is likely to produce substantial improvement in the objective function.

The accelerated research initiative that began in October 1986 has begun to address the important theoretical issues raised by Karmarkar's algorithm and other interior methods for optimization. It has also begun to overcome the obstacles to effective implementation. Over the next two years, it will apply these techniques to selected Navy problems.

There are intimate connections between Karmarkar's algorithm and several other areas of mathematics. Any iterative scheme can be viewed as a system of first-order differential equations by considering infinitesimal steps in the direction of the next iterate. Karmarkar's algorithm can thus be considered as a method of solving such a system. This analogy may lead to the construction of other algorithms based on higher order methods of solution. Karmarkar's algorithm is a nonlinear algorithm in that the projective transformation mentioned earlier creates a nonlinear objective function. As such, it is one of the few nonlinear algorithms with a proven global worst-case convergence bound. Extensions that yield a polynomial algorithm for quadratic programming have already been constructed. The relationship of Karmarkar's algorithm to other algorithms for nonlinear programming are being pursued in this initiative.

Since its conception 40 years ago, the simplex method has become an "engine" for optimization. A great many algorithmic structures have been built with this engine as the driving mechanism. To carry the analogy further, if the simplex engine is replaced by a Karmarkar engine, operating on different principles, these structures must be examined to ensure their compatibility. One of the most important of them is the body of algorithms that perform optimization over networks. These algorithms, together with specialized list-processing and modeling techniques, constitute one of the triumphs of operations research in the last decade. The translation from matrices and pivots to the language of nodes, arcs, and trees has profoundly affected our ability to solve many large, complex problems that, on the surface, bear little resemblance to networks. These translations are now being accomplished.

The last five years have also seen great progress in another technology that uses the simplex engine, integer programming, in which the solutions must have integral values. Current methodology is based on the solution of sequences of related linear programs. Depending on the techniques used, the elements in the sequence are related by addition of extra constraints or by the placement of additional bounds on the variables. In either case, the efficiency of these methods is crucially dependent on the use of information generated in the solution of the preceding elements of the sequence. Techniques are being developed for incorporating this information within interior methods.

Returning to the engine analogy, the simplex method has been fine-tuned over the years to operate very efficiently on routine problems and still be responsive in stressful situations. The performance of Karmarkar's algorithm, which has not had the advantage of such extensive development, becomes more impressive by comparison. Such comparisons may be misleading, however. Production LP codes are typically run at the beginning of each planning period, with the structure of the model unchanged but with changes in the data. The solution for the current period is usually close to that for the preceding period. The simplex method is able to start from the last solution, thereby greatly reducing the number of iterations required. No such advanced starts are yet possible with Karmarkar's algorithmn.

Sensitivity information concerning the optimal solution is often as important as the solution itself. The simplex method provides basic solutions, i.e., solutions that are at a vertex of the LP-polytope. This feature permits the computation of marginal costs—changes in the objective function corresponding to small changes in resource constraints. Interior methods, on the other hand, grow numerically unstable as they approach the boundary and thus cannot be used to obtain such sensitivity information. We are developing new algorithms to produce this required sensitivity information while staying within the interior framework.

The Navy shares large and complex planning problems with the commercial world. The research being supported under ONR's accelerated research initiative is intended to make the solution of such optimization problems much cheaper. This, in turn, may result in an even greater number of problems from such diverse areas as pattern recognition, engineering design, inverse methods, and signal processing being formulated as optimizations, thereby extending mathematical programming into new areas. The research is also intended to reduce the time needed to reach optimal solutions. If these efforts are successful, the importance of linear programming for real-time applications may come to equal its current preeminence as a planning tool.

Biography

Dr. Neal Glassman is a scientific officer in the Air Force Office of Scientific Research, Mathematics Division. His publications have been primarily in the area of operations research. He is a member of the Operations Research Society of America and the Military Operations Research Society. Formerly he was with the Office of Naval Research.

SILICON CARBIDE COMES OF AGE

Max N. Yoder, Office of Naval Research and
Robert F. Davis, North Carolina State University

Recent advances in the synthesis, growth, and processing of single crystal silicon carbide render it a promising material for advances in electronics and optical applications

Silicon and Carbon are among the most abundant materials on earth. While carbon is extensively used by nature in the molecular structure of most forms of life, both silicon and carbon are increasingly used in high technology applications. Silicon carbide (SiC) is the only intermediate phase in the Si-C equilibrium system at one atmosphere pressure. It does not occur in nature. The first reported synthesis was accidental—a result of attempts by Berzelius to make diamond. Acheson began the commercial manufacture of SiC in the United States. He also gave it the trade name "carborundum" from the combination of the Latin words carbon and corundum. Silicon carbide is also a generic name for several different materials that contain SiC and additional components and phases which have been consolidated into a solid body using different high temperature process routes. Collectively, these various materials possess a variety of microstructural relationships among the various phases which, in part, manifest control of the associated physical properties. In one or more of its polycrystalling forms, SiC is a principal candidate for high-temperature and/or high strength and and/or abrasion resistant applications, for instance, as heat exchangers in fossil fuel systems, critical parts for uncooled gas-turbine and adiabatic diesel engines and seals for pumps which move abrasive slurries.

Silicon carbide is also a semiconductor. Active devices have been produced in its high purity (or controllably doped) single crystal form. However it is only now that some of these devices are becoming commercially available. Some of their potential applications are in high-temperature,-frequency, and -power electronic devices; blue-light emitting diodes; Schottky diodes; UV radiation detectors; high-temperature photocells; and heterojunction devices. It is this aspect of SiC which is the focus of this paper.

Different crystal forms of the same chemical composition are called polymorphs. Polymorphism commonly refers to a three-dimensional change affected by either a complete alteration of the crystal structure or a slight shift in bond angle. Polytypism is a special type of polymorphism which occurs in certain close-packed structures. In this phenomenon, two dimensions of the basic repeating unit cell remain constant for each crystal structure (polytype), while the third dimension is a variable integral multiple of a common unit perpendicular to the planes in the material having the highest density (closest packing) of atoms. Silicon carbide has long interested crystallographers as a primary example of polytypism, for it has been determined to occur in more than 170 different one-dimensional ordering sequences without apparent variation in stoichiometry (however, recent data suggests that the Si/C ratio decreases as a function of the degree of hexagonality in the crystal until an exact 1:1 ratio is obtained at the completely hexagonal (2H) polytype).

The fundamental structural unit in all SiC polytypes is covalently bonded tetrahedron of four C atoms with a Si atom at the center. Each C is likewise surrounded by four Si atoms. The tetrahedra are linked through their corners, thus satisfying the four-fold coordination at any strucutural point and occupying an array of positions analogous to those occupied by spheres in close-packed structures. The simplest polytype notation is due to Ransdell, who assigned the letters C, H and R to represent the cubic, hexagonal and rhombohedral structures, respectively (the only crystallographic structures found in SiC) and combined them with a numeral which represents the number of closest-packed layers in the repeating sequency. The most common polytypes are 3C and 6H; 4H, 15R and 2H have also been identified in crystallite form, but are much more rare. All other polytypes are combinations of these basic sequences. The lone cubic polytype (3C) is also referred to as beta-SiC; the remaining polytypes are known collectively as alpha-SiC. Although a considerable body of literature exists regarding the kinetics and thermodynamics of polytype formation, growth, and stability, neither the physiochemical mechanism that produces the periodic sequences nor the forces leading to structures with very large unit cells are understood for this material. This literature does indicate that beta-SiC may be both the initial polytype that forms at virtually all temperatures and a necessary precursor to the occurrence of other polytypes, as a result of transformation. This polytype is particularly interesting from the standpoint of electronics.

A fundamental property of a semiconductor is the forbidden region (bandgap) in which charge carrier energies are not allowed. Beta-SiC exhibits an electronic band gap of 2.2 electron volts (eV) at 300°K. This is exactly twice that of the 1.1 eV exhibited by the most common semiconductor (silicon) and not closely approached by any other semiconductor in common use. This large bandgap exists primarily as a result of the high strength of the chemical bond between silicon and carbon. This larger bandgap manifests itself in several ways. The most obvious one is that unlike common semiconductors, beta-SiC is transparent to light at wavelengths longer than 516 nanometers. Thus, while it absorbs blue and green light, it transmits red light very well. Between red and green in the spectrum lies yellow which is partially transmitted and partially reflected by beta-SiC. Figure 1 illustrates a film of beta silicon carbide lying over graph paper. The film is only 20 micrometes thick—about one half as thick as a human hair and was grown on and subsequently removed from a silicon substrate by the NASA Lewis Research Center.

Figure 1

Free-standing beta-Sic films courtesy NASA Lewis Research Center

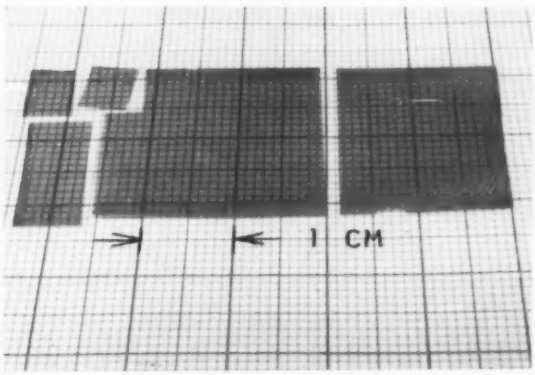

The larger bandgap exhibited by beta-SiC also translates to a much higher dielectric strength (electric field at which breakdown occurs). For SiC this number is 4 million volts/cm or ten times that of the common gallium arsenide semiconductor and 13 times that of silicon. Since the output power which a semiconductor transistor is capable of delivering is proportional to the square of the voltage swing across that transistor, SiC is theoretically capable of delivering 100 times the output of a gallium arsenide device and 169 times that of a comparable silicon device. Another attribute of the higher bandgap is its thermal properties. As a semiconductor is heated, its electrons gain energy with the result that an increasingly larger number are transferred from the valence band to the conduction band. Since this number is inversely proportional to an exponential function of the bandgap, SiC transistors and diodes can be operated at a much higher temperature than can devices of common semiconductors. A striking example of this is shown in Figure 2. Here a beta-SiC transistor is shown under test at 650 degrees Celsius. At this temperature it glows red hot. This is fully 250 degrees hotter than any other transistor has ever been shown to operate! The current versus voltage characteristics of the transistor are shown in Figure 3. Several aspects of SiC transister performance are notable. First, the curves have large horizontal sections which means that the output conductance is low—a very desirable property for an amplifier. Second—and most unique, is that the highest performance is obtained at temperatures in excess of 300°C. No other known semiconductor increases its performance as a function of increasing temperature above its room temperature performance. Finally, performance at 650°C is nearly as good as room temperature performance. This capability has rather profound implications. Aside from such down-to-earth applications as better control over (1) thermal appliances such as hair dryers, electric irons, and space heaters and (2) various functions

such as the air/fuel mixture in carburetor of automobiles, the space program could benefit substantially. Many satellites devote over 50% of their volume and weight to various forms of cooling equipment to cool their electronics to temperatures below that of boiling water. It can be shown that entire cooling systems in unmanned satellites can be eliminated if electronics can be found which will operate at temperatures in the vicinity of 350 degrees Celsius. Not only could the satellite be simplified with commensurate reliability improvements, but launching costs for the reduced payload weight could be substantially affected.

Figure 2

SiC transistor glowing red-hot at 650 C

Related to the high temperature operation of electronics is the reliability of the semiconductors themselves. As temperatures increase, the impurities used to dope the semiconductors move or diffuse at proportionally higher rates. Since the boundaries of these impurities are what define the transistors and other devices made in the semiconductor, the properties of the semiconductor begin to change with impurity diffusion and the device can no longer perform its intended function. The extremely strong bond between silicon and carbon in the SiC crystalline lattice structure greatly inhibits the diffusion of impurities. Figure 4 shows the diffusion of various impurities in SiC. The very impressive feature is that at temperatures well above 1423 °C wherein the common silicon semiconductor melts, impurities in SiC are still rather stable! GaAs melts at an even lower temperature of 1220 °C. Thus the typical diffusion dominated wear-out mechanism found in GaAs power transistors is not present in SiC at measurable rates.

The dielectric constant of a semiconductor helps to set the upper operating frequency of a device made from that material. In contrast to a dielectric constant of 11.8 for silicon, 12.8 for gallium arsenide, and 14 for indium phosphide, beta-SiC exhibits a dielectric constant of only 9.72. This lower value significantly reduces capacitive parasitic losses associated with the charging/discharging of transmission lines in circuits fabricated of SiC, and enables the reduction in size of the transistors needed to drive electrical signals down the microminiature transmission lines interconnecting the transistors on chip and between chips. The decreased size further reduces power requirements and reduces power supply size and cost.

Figure 3

SiC transistor characteristics at 300 C and 650 C

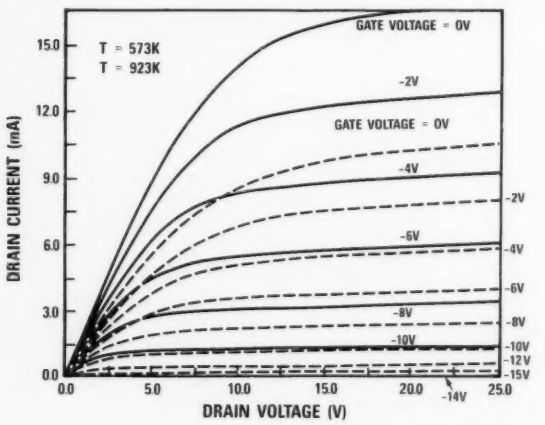

The ability to dissipate heat is not only proportional to the temperature difference between the source and the sink (the efficacy of SiC to satellites), but is also proportional to the thermal conductivity of the material itself. Here SiC is also a winner. At room temperature its thermal conductivity is equivalent to that of copper (5 watts/cm-°C). This compares to values of 1.5 and 0.5 for silicon and gallium arsenide, respectively. Thus while SiC can operate reliably at elevated temperatures (unlike common semiconductors), its high thermal conductivity also ensures that heat is adequately dissipated from the device.

Figure 4

Impurity Diffusion in SiC as a function of temperature

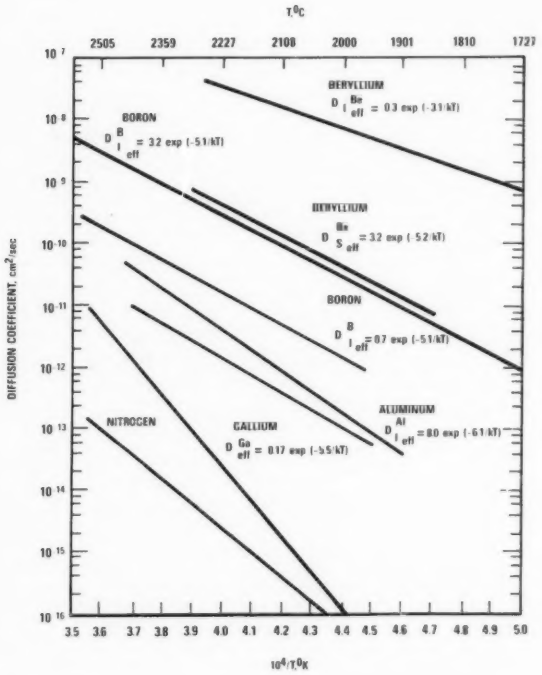

The velocity of the charge carriers (e.g., electrons and holes) in a semiconductor typically varies as a function of the electric field strength to which the carriers are subjected. In gallium arsenide and related III-V semiconductors this velocity can be very high for even comparatively low values of electric field. This engenders devices made of these materials to exhibit very high frequency response at low signal levels. As signal levels increase and the required electric fields within the semiconductor increase proportionately, these materials lose their low field velocity advantages, as shown in Figure 5. Figure 6 provides a major part of the explanation for this phenomenon. Shown in red is the band diagram for gallium arsenide. Gallium arsenide is a direct bandgap material in that the minimum of the conduction band occurs at the same point in "k" space (a manner of illustrating momentum of charge carriers) as does the maximum of the valence band. As electrons in conduction band valley gain energy they are driven to the subsidiary conduction band valley where the parabolicity is less and their effective mass is greater. With the same energy, they must slow down in accordance with the formula for kinetic energy. In contrast, SiC (like silicon) is an indirect bandgap material in that its conduction band minimum does not lie in the same point in k space as does the valence band maxima. In SiC, the low parabolicity of the conduction band causes the electrons to be comparatively heavy and thus (for any given energy level) slower than electrons in gallium arsenide. Unlike electrons in gallium arsenide, however, electrons gaining energy in SiC can transfer to an upper subsidiary conduction band wherein the parabolicity is somewhat greater and the effective mass is somewhat lower thus causing them to gain velocity. In this respect, SiC is no different from silicon. As electrons gain further energy, however, they are scattered by their interaction with optical phonons. In both silicon and gallium arsenide this scattering limits electrons to a velocity of 10 million cm/sec. In beta SiC, the lighter mass of carbon causes this limit to occur at a velocity 2.5 times greater. Thus while both silicon and gallium arsenide exhibit greater velocity at low electric field, SiC is clearly superior at high electric fields.

Figure 5

Velocity-field comparison of SiC with Silicon and GaAs

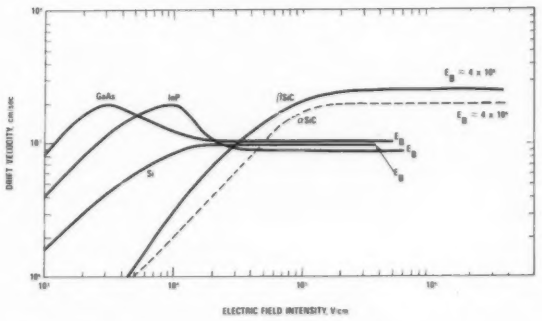

High charge carrier velocity at high electric fields is very important in two different types of electron device applications. The first is in power devices operating in the microwave and millimeter wave spectrum. To obtain high power at microwave frequencies, the high carrier velocity must be present at high electric fields. The very high electric field breakdown (dielectric strength) of SiC enables large voltage changes simultaneously with high carrier velocity. Figure 5 illustrates the order of magnitude superiority of SiC in this respect. To be able to operate at frequencies in the millimeter wave spectrum, the velocity of the electrons must be high.

Figure 6

Band Diagrams for GaAs and SiC

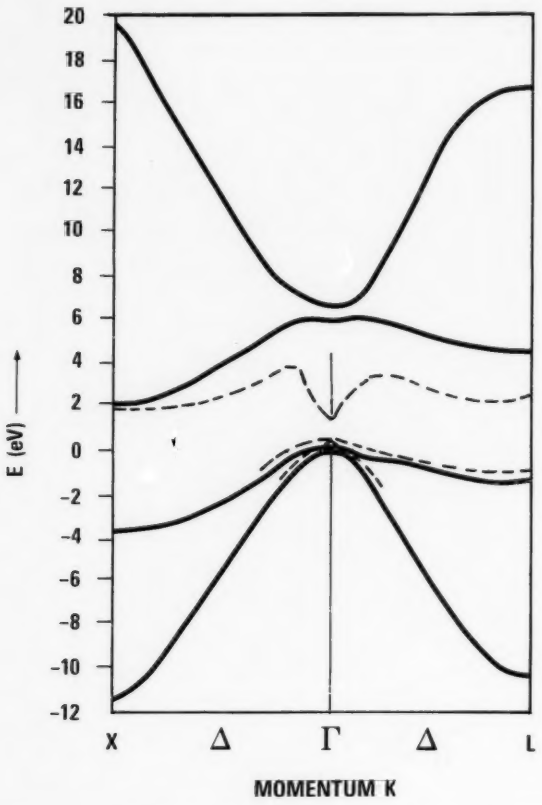

It is seen in Figure 5 that electrons in silicon can never reach the velocity-field product required for microwave power amplifiers (2×10^7 cm/sec and 5×10^4 volts/cm). While gallium arsenide meets the velocity requirements for low electric field strengths, it falls short at the higher fields needed for high power amplifiers or oscillators. Over two decades ago and prior to any serious attempts to synthesize semiconducting grade SiC, A. Johnson published a method for selecting the proper semiconducting material for high performance electron devices. Table I is derived from those criteria and compares various candidate semiconductor materials. The potential of SiC is striking!

The second type of electron device wherein high charge carrier velocity at high electric field strength is clearly an attribute is that of high density integrated circuits. As the density of logic functions per unit area increases, individual transistor size must decrease as indeed it has done over the past four decades. Decreased transistor size also provides a shorter path length (channel) for the electrons to transit between the transistor source and drain as shown in Figure 7a. Owing primarily to noise margin limitations, logic swing levels (voltage levels between a logic 0 and logic 1) must be maintained at several volts. (Typical logic levels today vary between 0 and 5 volts.) With the applied voltage fixed and the transistor channel length decreasing, the internal electric fields continue to increase. State-of-the-art transistors exhibit one micrometer channel lengths. At this value it is seen from Figure 5 that both silicon and gallium arsenide exhibit saturated velocities of but 10 million cm/sec whereas SiC still exhibits a positive mobility (velocity versus field slope) and is comfortably far from its breakdown limits. In 1972, R.W. Keyes developed a figure-of-merit for the selection of a semiconductor material for use in dense integrated circuits. Factors used by Keyes include dielectric constant, thermal conductivity and saturated velocity—in all of which SiC excels. Table II has been compiled based on the criteria of Keyes. From it, there are strong reasons to use SiC in integrated circuit development.

The low field mobility (velocity versus field slope) of silicon carbide is lower than that of common semiconductors as shown in Figure 5. While that could be interpreted as a serious disadvantage for devices manufactured only 5 years ago, present generation micrometer-dimensioned electron devices are much more dependent on saturated velocity than on low field mobility. Even newer device configurations may provide a decided advantage to SiC. One such configuration is shown in Figure 7b. This device is known as a dual gate field effect transistor (FET) wherein electrons transit from the source to the drain and are modulated by the gates.

Table I.
Johnson Figure of Merit

	E(BD)	V(sat)	$\frac{E(BD)*V(sat)}{\pi}$	Pwr*Freq² *Imped	Ratio
	volts/cm	cm/sec	volts/sec	$\frac{\text{Watt-Ohms}}{\text{Sec}^2}$	
	x10⁵	x10⁷	x10¹¹	x10²³	
MATERIAL					
Silicon	3	1.0	9.5	9.0	1.0
GaAs	4	2.0	25.0	62.5	6.9
InP	6	2.0	38.0	144.4	16.0
SiC (alpha)	40	2.0	250.0	6250.0	694.4
SiC (beta)	40	2.5	320.0	10240.0	1137.8

Table II.
Keyes Figure of Merit

Material	T	V(sat)	K	$T(\frac{\sqrt{V(sat)}}{K})$	Ratio
Units	@ 300K W/cm°	cm/Sec x10	dimensionless	W/cm/sec° C x10²	
Silicon	1.5	1.0	11.8	13.8	1
GaAs	0.5	2.0	12.8	6.3	0.5
InP	0.7	2.0	14.0	8.4	0.6
SiC (beta)	5.0	2.5	9.7	90.3	5.8

In theory, the dual gate device provides much higher gain and much better output conductance than does a single gate device. When fabricated in gallium arsenide, electrons under the second gate and beyond are in their heavy mass, lower velocity state as their energy levels are high. As such, the second gate cannot be used to modulate the device at microwave frequencies. In SiC, however, electrons transiting under the second gate are at their very fastest velocity. In fact, the AVERAGE velocity of the electrons in the SiC device is expected to be substantially higher than in the gallium arsenide device. In this respect, the dual gate FET effectively circumvents the lower low field mobility of SiC. If the first portion of this dual gate SiC FET is used solely as an electron injector for the second part of the device, and the overall device is submicrometer so as to further reduce the probability of electron scattering, then not only will the average velocity of electrons be much greater than that of electrons in most common semiconductors, but the electrons will all be traversing at velocities nearly equal to each other. If such can be verified, SiC (contrary to intuition) could also exhibit a very low noise background and thus compete with the now-dominant gallium arsenide devices in this application.

Other reasons for choosing SiC are related primarily to immunity to radiation damage and to burn out from electromagnetic pulses (EMP) such as those originated by lightning. While no measurements have yet been conducted to verify the immunity of SiC circuits to EMP damage, the intrinsic advantages of higher dielectric strength and higher thermal conductivity will certainly be beneficial. Recent cobalt 60 gamma ray measurements have shown SiC field effect transistors to be unaffected to total doses exceeding 10^7 RADS.

Figure 7

(a) Single gate Field Effect Transistor
(b) Dual gate Field Effect Transistor

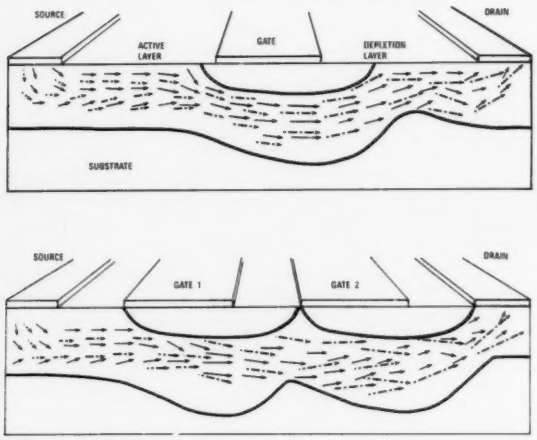

Figure 8

Optical Reflectivity of SiC

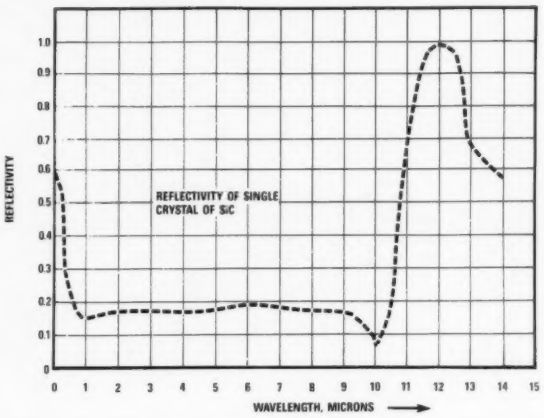

Optical Properties. Microparticle abrasion is a serious problem in many optical lenses, mirrors, and windows. The hardness of SiC makes it potentially useful in airborne, spaceborne, and related applications. The optical reflectivity of SiC is shown in Figure 8. Although it has strong reflectivity at 12 micrometers, through the optical spectrum of 0.6 to 10 micrometers, it is quite acceptable for use as a window. Undoped SiC in its alpha form is transparent and colorless, but aluminum doping turns it blue and boron doping colors it brown. Beta-SiC (as was earlier mentioned) is yellow because of its bandgap, but the addition of nitrogen impurities tends to color it green. Hexagonal 6H material that is nitrogen doped is green; whereas, undoped 6H material is colorless. The index of refraction of the cubic beta material is 2.48 while that of the hexagonal material tends toward 2.7.

Nucleation, Synthesis, and Growth. Many of the above-stated properties and applications of SiC have long been known, but the required SiC materials simply could not be produced in the required perfection, quantities, and yields. During 1987/8 most of these limitations have been overcome. The most significant of these was the synthesis and reproducible growth of single crystal SiC boules of the 6H hexagonal type via sublimation growth techniques. Another important factor in the growth of usable SiC boules was the improvement in purity of the starting materials. A porous cylinder of graphite is coaxially located inside an outer, nonporous graphite clyinder. Between the two is placed a mixture of high purity powdered silicon and carbon. The seed crystal is placed inside the porous cylinder and the entire apparatus is brought to a temperature of 2250°C with a temperature gradient in the vicinity of the seed which is maintained as the coolest part of the apparatus. Monocrystalline boules of 6H SiC grown from this apparatus have exhibited crystalline defect densities as low as $10^4/cm^2$—similar to that of gallium arsenide crystals used today. Figure 9 depicts one such boule. Although current boule diameters are no larger than 2 cm in diameter, 2 inch diameter boules are under active development. Even then, the 2 cm diameter boules provide material adequate in size to serve as windows and suitable for use in electron device development.

While the process has not yet been perfected to grow SiC boules of cubic crystalline structure, research directed toward that pursuit is currently underway. Cubic SiC films have been epitaxially grown on the hexagonal substrates. When the 6H boules are cut into wafers such that the basal plane (c-axis) is the wafer surface, cubic SiC is grown by chemical vapor deposition methods flowing silane and ethylene gases carried in H_2 over the wafer at temperatures in the vicinity of 1400°C. In this juxtaposition orientation the crystallographic axes of the growing cubic and the underlying hexagonal crystals perfectly align as shown in Figure 10. Here the interface between the hexagonal substrate and the cubic epitaxial layer is viewed using high energy, high resolution transmission electron microscopy. The layered hexagonal underlying crystalline structure is easily discernable from the overlying epitaxial cubic film. The atoms of each crystal are seen to be perfectly aligned at the interface. Should the surface of the underlying 6H hexagonal wafer be misoriented more than 2 degrees off the basal plane, only hexagonal epitaxial films of 6H–SiC can be grown.

Figure 9

6H SiC crystal boule

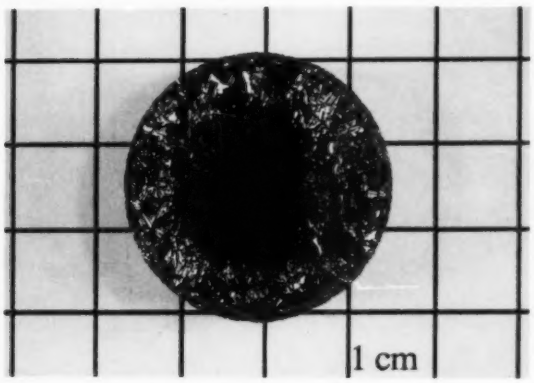

Figure 10

Cubic SiC on hexagonal SiC Interface

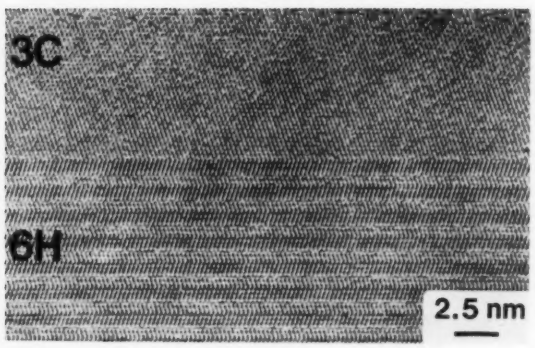

Summary. While SiC is clearly superior to the conventional semiconductors in many critical respects and it has at last (in small size) been produced with perfection as good as what is now commonly used in the gallium arsenide industry, much remains to be done. The investment in SiC to date is less than 1% of the total investment in gallium arsenide which, in turn, has only experienced a few percent of the investment experienced in silicon. Although processing of a material with the hardness of SiC is difficult, it is not without advantages in that it is not easily damaged during manufacture. In this respect industrial yield may ultimately exceed that of gallium arsenide. If past continues to be prologue we can expect that the established semiconductor industry will not espouse SiC. Just as the established germanium industry left newcomers to exploit silicon, and the silicon industry left newcomers to exploit gallium arsenide, the SiC industry is expected to grow from newly-formed industries championing its cause. Even then, we can expect to see the first SiC electronic products in everyday use early in the next decade.

Biographies

Max Yoder is an electronics engineer with the Solid State Electronics Branch of the Office of Naval Research (ONR) where he supervises programs in semiconductor materials, monolithic microwave integrated circuits, gigabit logic, new electronic device structures, and electromagnetic system applications. He has published and presented many papers in these fields of solid state materials. He is a pioneer in the development of research programs for monolithic microwave devices in the U.S. Currently he manages at ONR the research program in diamond semiconductor technology.

Dr. Robert Davis is Professor of Materials Science and Engineering at North Carolina State University. His research and papers have been in the fields of thin films for microelectronic devices, self-diffusion of ^{14}C and ^{30}Si. and high temperature creep in silicon carbide. He is a Fellow of the American Ceramic Society and recipient of the ALCOA Distinguished Research Award.

Navy Honors Dr. Fred Saalfeld for Science Research Management

The Honorable Thomas F. Faught, Jr., (left)Assistant Secretary of the Navy for Research, Engineering and Systems, presented the Conrad Award for 1988 to Dr. Fred E. Saalfeld, Director of the Office of Naval Research, who is accompanied by Mrs. Saalfeld.

Dr. Fred E. Saalfeld, Director of the Office of Naval Research (ONR), is this year's recipient of the U.S. Navy's Robert Dexter Conrad Award, the highest Navy honor for scientific achievement.

The award, in the form of a gold medal and a certificate, was presented to Dr. Saalfeld by Thomas F. Faught, Jr., Assistant Secretary of the Navy for Research, Engineering and Systems, during a ceremony in the Office of the Chief of Naval Research.

The Conrad Award is presented annually to an individual who has made outstanding contributions in the field of research and development for the Department of the Navy. It commemorates Captain Robert Dexter Conrad who was one of the primary architects of the Office of Naval Research. the R&D organization responsible for the basic research programs of the Navy.

Dr. Saalfeld has been working for the Navy since 1962 when he joined the Naval Research Laboratory (NRL), a field activity of the Office of Chief of Naval Research. At NRL, he worked as a bench chemist, head of the Mass Spectrometry Section, then as head of the Physical Chemistry Branch. In 1976, he became Superintendent of the Chemistry Division. During his tenure as Superintendent, he also served as Chief Scientist of ONR's Branch Office in London.

Dr. Saalfeld was appointed Director of the ONR Contract Research Department in 1982 and Associate Director of ONR in 1985. In 1987, he became Director of the Office of Naval Research .

Mr. Faught praised Dr. Saalfeld for his exceptional contributions and outstanding career as a scientist and manager. In presenting the award. Mr. Faught said of Dr. Saalfeld's work:

"... As a bench scientist and science manager in the Naval Research Laboratory's chemistry program. Dr. Saalfeld developed the Central Atmosphere Monitoring System (CAMS), now in service on the Navy's nuclear submarines, and was instrumental in developing new secondary ion mass spectroscopy techniques that are widely used today in molecular biology and medical research. As Director of the Office of Naval Research, Dr. Saalfeld has aggressively stressed and strengthened the scientific excellence of the Navy's Basic Research Program. His innovative management initiatives, exceptional scientific leadership, and outstanding management accomplishments have confirmed the position of the Office of Naval Research as a leader among federal agencies. His distinguished scientific achievements, exemplary management of research programs, and commitments to scientific excellence have directly contributed to the development of major new operating capabilities for the United States Navy."

Dr. Saalfeld is the 33rd recipient of the Conrad Award. Other awards and honors he has received include the Presidential rank of Meritorious Executive, the Navy Superior and Meritorious Civilian Service Awards, and the Navy Superior Merit Award.

Dr. Saalfeld is Founder and First President of the Mass Spectrometry Discussion Group of Greater Washington, Past National Councilor of the American Chemical Society, Past Secretary of the American Society for Mass Spectrometry, and member of 14 national and international professional societies.

He has authored over 450 scientific papers. reports and presentations and has patents for three scientific inventions.

A native of St. Louis, MO, Dr. Saalfeld obtained his Ph.D. from Iowa State University, and his B.S. from Southeast Missouri State University from which he received the Alumni Merit award in 1988.

Superconductors for the Navy

Superconductivity, the transport of electrical current without energy loss due to resistance, and the devices that use this phenomenon are now leading topics in scientific and technological circles, including the Navy. The Navy never ignored the possibilities of superconductivity: quite to the contrary. For example, the Office of Naval Research (ONR), since its founding in 1946, has supported superconductivity research.

That year, ONR sponsored two conferences for scientists it supported at universities and in industry who were working in the field of superconductivity. From this meager beginning, ONR became a focal point for much of the low temperature physics and superconductivity research in the United States. Today, it manages some $22 million in Navy and Defense funds in this area.

The interest today stems from the discovery, in 1986, of high-temperature superconductors. This important breakthrough occurred when scientists at IBM Zurich reported a material which became superconducting at temperatures as high as 30K(-243C). Soon after scientists at the University of Alabama and Houston discovered a material which superconducts at 90K(-183C).

These new materials give hope to such forecasts as: trains levitated by magnetic forces: powerful, small and cheap computers; techniques for reading brain cell signals; electric cars; and electric motors which are half the size, weight, and cost of motors today.

The phenomena of superconductivity was first recognized in 1911 when the Dutch physicist Kamerlingh Onnes noted that as he cooled mercury to the temperature of liquid helium (4K) the electrical resistance of the mercury dropped suddenly from a finite value to zero. He concluded that mercury had passed on to a new state, which because of its extraordinary electrical property, he called the superconducting state. Since then scientists have discovered that upon cooling, the zero electrical resistance state can be produced in about 1,000 elements, alloys and compounds, including such common metals as lead and tin, as well as a few exotic organic compounds. The temperature at which material transforms from its normal resistance state to a state of perfect electrical conductivity is called its transition temperature, T_c.

The transition temperature of most superconductors is very low, and because of this, the practical applications of superconductivity have been extremely limited. Over the years, the T_c of newly discovered superconductors has risen very slowly, until recently the highest known T_c was only 23K in the compound Nb_3Ge. Then in 1986, came the news of high-temperature superconductors producing a quantum jump in T_c that will bring revolutionary results to the field, according to Dr. Donald Gubser who heads the superconductivity program at the Naval Research Laboratory (NRL) in Washington, DC.

For the Navy, ONR's long term commitment to low temperature physics has already helped produce ultrasensitive, low noise, magnetic and electromagnetic detectors, electric drive systems currently under evaluation for ship propulsion, and ultra high speed electronic logic and memory circuits, all based on superconductivity. Civilian applications include magnetocardiography, magnetoencephalography, and some 600 large supermagnets which are essential components of magnetic resonance imaging systems which are revolutionizing noninvasive medical diagnosis. Other applications include the more than 1,000 supermagnets that guide protons around the four mile circumference of the Fermi Laboratory's particle accelerator and enormous supermagnets for the confinement of plasmas to achieve controlled thermonuclear fusion.

ONR now supports research programs at NRL for developing the new high T_c superconducting materials discovered in 1986 and a variety of processing techniques to further improve their properties. These new materials are made by mixing oxides and carbonates of yttrium, barium, and copper, pressing into shape, and sintering at 1000C in a platinum crucible to form bulk samples. The samples are then tested for superconductivity by cooling in a special dewar where the electrical resistance is measured as a function of temperature. These samples are used to test a variety of properties and to understand the materials from a microscope point of view. According to Dr. Gubser, the arrangement of atoms in the materials as well as their high transition temperature suggests that new mechanisms may produce a host of novel physical properties in these materials. He claims that "scientists must reexamine many of their long held concepts about the mechanisms producing superconductivity as well as the materials where it is most likely to occur."

From a technological viewpoint, the new materials will permit applications of superconductivity with much simplified refrigeration systems. Many superconductivity applications will now become technologically and economically viable options for a variety of uses. And in those cases where superconductivity is the only available option for an emerging technology, these new materials will speed the development due to the significant easing of the refrigeration requirements.

These superconductors, with critical transition temperatures above 77K (typical of a liquid nitrogen cryogen or a space environment), have caused the Navy RDT&E community to reconsider use of superconducting components and devices. Potential areas for applications of these would include, antisubmarine warfare; antisurface warfare; antiaircraft warfare; and command, control, communications intelligence. Here they may: (a) perform the same function as previously known superconducting devices but at a more easily achievable temperature, (b) perform functions of devices which used older, low T_c materials as above but better, or (c) perform entirely new functions, thus opening a broad array of opportunities for naval warfare systems.

The U.S. Navy has capitalized on its many years of research in superconductivity and materials in rapidly responding to these opportunities. Its current program is directed at both a basic understanding of these new materials and their application.

Tech Base Notes

Described below is a synopsis of recent technology accomplishments sponsored by the Office of Naval Technology, which is the Navy research and development (R&D) organization responsible for conducting the exploratory development (6.2 category) for the Navy. Exploratory development programs are conducted in industry, academia and in the Navy's own R&D centers.

Corrosion Protection for Aircraft Components

Naval aircraft structures that are subjected to high temperatures experience a high degree of corrosion and require frequent replacements of expensive components. Under Office of Naval Technology (ONT) sponsorship, the Naval Air Development Center has developed an organic coating that is thermally stable up to 700° F and provides corrosion protection far superior than materials currently used in military aircraft. This coating air dries at room temperature and is compatible with both steel components which are subjected to extreme heat. The new material consists of a protection by both the formation of a barrier layer and a chemical reaction on the substrate. The material is currently being tested by the Naval Air Depot A-4 and SH-60 aircraft. In addition, samples are being evaluated by General Dynamics and McDonnell Aircraft Company for use on various other Navy aircraft.

Reducing Shipboard RF Radiation Hazards

In the confines of a shipboard environment, RF transmissions can cause severe health-related effects to personnel as well as hazards of electromagnetic radiation to ordnance (HERO). Under Office of Naval Technology (ONT) sponsorship, the Naval Ocean Systems Center has developed a method to calculate near field RF radiation for shipboard antennae which will be useful in reducing hazards. Digitized input of geometries from blue prints, isometric display of ship system models and graphics-mode editing of isometric images used in conjunction with this calculation method will expedite the assessment and redefining of operation practices and the redesign of modification of antenna site plans. These reconsiderations of restricted area designations and antennae locations will prevent certain health hazards and minimize HERO unsafe conditions. The American National Standards Institute standard recently adopted by the Navy is much more restrictive than the previous standard, especially for the HF (2 to 30 MHz) band. This efficient, accurate prediction capability and anticipated long-term medical cost savings make the method cost effective; the Naval Sea Systems command is using it to assure compliance with the new standard.

NO POSTAGE
NECESSARY
IF MAILED
IN THE
UNITED STATES

BUSINESS REPLY CARD

FIRST CLASS PERMIT NO. 12503 WASH., D.C.

POSTAGE WILL BE PAID BY DEPARTMENT OF THE NAVY

Editor
Code OOPARI
Office of the Chief of Naval Research
Arlington, VA 22217-5000

DEPARTMENT OF THE NAVY
OFFICE OF NAVAL RESEARCH
ARLINGTON, VA 22217

OFFICIAL BUSINESS
PENALTY FOR PRIVATE USE, $300

THIRD CLASS MAIL
POSTAGE & FEES PAID
USN
PERMIT NO. GS-9

Important Renewal Notice

(Does not apply to paid subscription readers)
(Send entire back cover, folded as indicated, with mailing label attached)

FOLD FOLD FOLD

Readership Survey

Navy publications and printing regulations require that all mailing lists be verified at least once a year to identify incorrect addresses and addressees who no longer qualify for free distribution.

Please indicate if you want to continue receiving *Naval Research Reviews* and add any comments you may have about the publication. We will consider these comments in planning future issues. Also, indicate any changes of address below the label, and make sure the label is returned with this survey. Fold this sheet and staple to reveal NRR address.

Addressees whose response does not reach the *Naval Research Reviews* Editor by October 1, 1989, will be removed from the mailing list.

Please Complete the following

1. ☐ I want to continue receiving Naval Research Reviews.

2. ☐ Please remove me from the mailing list.
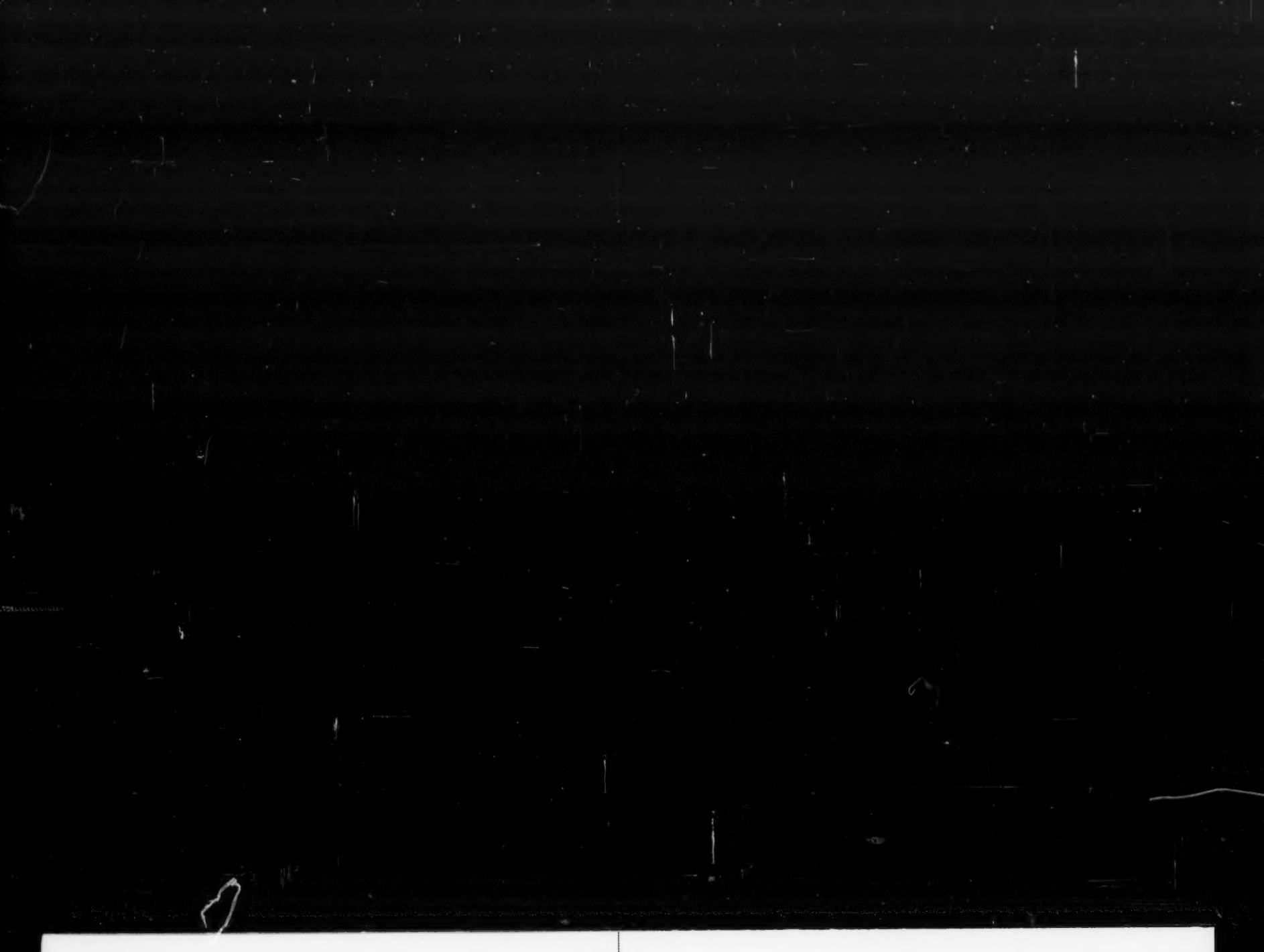
Comments: